*Journal of Paleontology*, 93(4), 2019, p. 798–821

0022-3360/19/1937-2337
doi: 10.1017/jpa.2019.11

JOURNAL OF PALEONTOLOGY
A PUBLICATION OF THE Paleontological SOCIETY

# Cranial and post-cranial remains and phylogenetic relationships of the Gondwanan meiolaniform turtle *Peligrochelys walshae* from the Paleocene of Chubut, Argentina

Juliana Sterli[1,2] and Marcelo S. de la Fuente[1,3,4]

[1]Consejo Nacional de Investigaciones Científicas y Técnicas (CONICET), Argentina
[2]Museo Paleontológico Egidio Feruglio. Av. Fontana 140, Trelew (9100), Chubut, Argentina <jsterli@mef.org.ar>
[3]Museo de Historia Natural de San Rafael, Av. Balloffet S/N° frente al Parque Mariano Moreno, 5600 San Rafael, Mendoza, Argentina
[4]Instituto de Evolución, Ecología Histórica y Ambiente (CONICET-IDEVEA-UTN FRSR), Calle Urquiza 314, 5600 San Rafael, Mendoza, Argentina <mdelafuente@mendoza-conicet.gob.ar>

**Abstract.**—*Peligrochelys walshae* is a meiolaniform turtle originally described based on four specimens represented by cranial remains found in the classic locality of Punta Peligro (Chubut, Argentina) in outcrops of the Salamanca Formation (Danian). Recent field work in the vicinity of Punta Peligro resulted in the discovery of almost 30 new specimens, represented by cranial and postcranial remains that can be assigned to *P. walshae*. In this contribution, we provide a detailed anatomical description of the new specimens, provide an emended diagnosis for the species, and explore its phylogenetic relationships based on all anatomical data available for the species. The new specimens bring valuable information about the anatomy of the skull and postcranium of *P. walshae* as well as for meiolaniforms in general. The 3D preservation of the skull bones allows us to provide a 3D reconstruction using novel techniques. The updated phylogenetic analysis confirms that *P. walshae* is part of the clade Meiolaniformes, which spans from the Early Cretaceous until the Holocene and contains the giant, horned turtles (Meiolaniidae). This phylogenetic analysis reinforces the previous hypothesis that the clade Meiolaniformes is dominated by Gondwanan taxa, but also includes some Laurasian representatives. Alternate phylogenetic positions of taxa included in Meiolaniformes in this analysis were tested using the Templeton test. The lineage leading to *Peligrochelys walshae* is the only meiolaniform non-meiolaniid lineage to have survived the K-Pg mass extinction; its study provides valuable information to evaluate the effects of the K-Pg extinction in turtles.

## Introduction

Meiolaniformes is a clade uniting all the forms closely related to the giant, terrestrial, highly ankylosed turtles with frills and horns in the skull and tails bearing rings and clubs grouped in Meiolaniidae. Meiolaniforms are known, at least, since the Early Cretaceous until the Holocene (Sterli and de la Fuente, 2013; Sterli, 2015; Sterli et al., 2015a). Their phylogenetic content is controversial. For some authors (e.g., Sterli et al., 2015a), Meiolaniformes is a clade that mainly includes forms from South America and Australasia, with some members from Europe and Asia. While for other authors (e.g., Joyce et al., 2016), Meiolaniformes contains only Gondwanan forms.

*Peligrochelys walshae* Sterli and de la Fuente, 2013 has been always recognized as a member of Meiolaniformes (Sterli and de la Fuente, 2013; Joyce et al., 2016). This taxon was named by Sterli and de la Fuente (2013) based on four specimens represented only by cranial remains recovered in outcrops of the Salamanca Formation (Danian) at the Punta Peligro locality (Chubut, Argentina). In this contribution, we present several new specimens assigned to *P. walshae* coming from several sites in the vicinity of the Punta Peligro locality. All sites are located in the same horizon within the Salamanca Formation (Danian). The new specimens are represented by cranial and postcranial remains providing new anatomical information about this taxon. All bones from the skull were 3D scanned and a 3D cranial reconstruction is provided for the first time for this taxon. Furthermore, we performed a renewed cladistic analysis to test the phylogenetic position of *P. walshae* among turtles.

## Materials and methods

*Materials.*—All specimens described in this work are housed at the Museo Paleontológico Egidio Feruglio (Trelew, Chubut, Argentina). Most of the materials were collected during two field trips in 2013 and 2014. The materials collected in those years are generally associated with a field number and precise locality information (continuous circles in Fig. 1), with the exception of some specimens (dotted circle in Fig. 1). The remaining specimens were collected in 2002 and 2004 by a team lead by G. W. Rougier (University of Louisville). These specimens (MPEF-PV 10909–10912, 10917) lack locality information beyond the Punta Peligro area (dotted circle in Fig. 1).

The description provided in this work is based on the following specimens (see also Supplementary Data 1).

MPEF-PV 10831.—Right frontal, left and right postorbitals, right and left quadrates, left quadratojugal, left and right exoccipitals, neural arch of cervical vertebra 3, cervical vertebrae 4

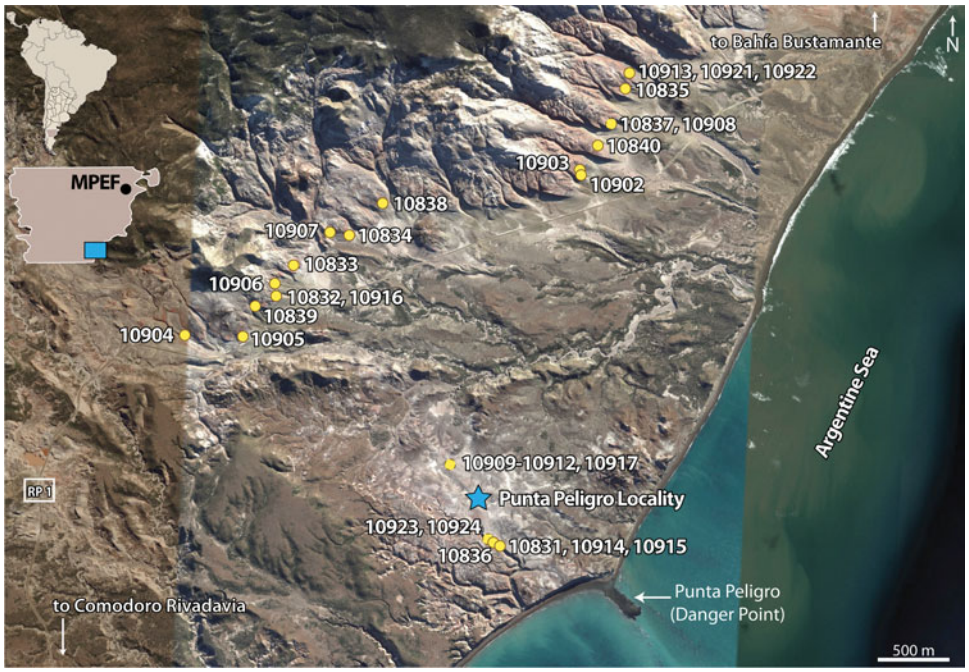


**Figure 1.** Map showing the location of each specimen in the vicinity of Punta Peligro Locality, Southeastern Chubut, Argentina. Continuous circle, specimens with precise location; dashed circle, specimens with no precise location; star, traditional Punta Peligro Locality; MPEF, location of Museo Paleontológico Egidio Feruglio, Trelew, Chubut where all the specimens shown in the map are housed; RP, provincial route. Google Earth Pro v 7.1.8.3036 (January 17, 2017), South East Chubut, Argentina. Data SIO, NOAA, U.S. Navy, NGA, GEBCO. DigitalGlobe 2018 and TerraMetrics 2018. http://www.earth.google.com (September 20, 2018). Scale bar equals 500 m.

and 7, medial thoracic vertebra and thoracic vertebra 9, sacral vertebra 2, 12 caudal vertebrae, nuchal bone, neural bone, left and right peripherals 1, left peripheral 2, last left bridge peripheral, indeterminate plastral fragments, left scapula, proximal end of left coracoid, proximal and distal ends of left humerus, one left metacarpal, two phalanges, one ungual phalanx, right femur, distal end of left tibia, and left astragalocalcaneum.

MPEF-PV 10832.—Right premaxilla, right jugal, left and right frontals, left postorbital, right prootic, left and right opisthotics, left exoccipital, left and right quadrates, left dentary, neural arch of the atlas, cervical vertebra 3, several peripherals, two neurals, indeterminate plastral remains, a distal portion of a metacarpal or metatarsal, and one phalanx.

MPEF-PV 10833.—Right jugal, left quadrate, basisphenoid, peripheral 1, and a neural.

MPEF-PV 10834.—Right postorbital, nuchal, right peripheral 3, sacral vertebra 2, right scapula, and an osteoderm.

MPEF-PV 10835.—nuchal bone, 2 caudal vertebrae, proximal end of left humerus, and distal end of left radius.

MPEF-PV 10836.—Nuchal, left peripheral 3, bridge peripheral, a caudal vertebra, and proximal and distal ends of right humerus.

MPEF-PV 10837.—Fragment of nuchal bone.

MPEF-PV 10838.—Anterior part of left dentary and nuchal.

MPEF-PV 10839.—Nuchal and left peripheral 1.

MPEF-PV 10840.—Right peripheral 1, left peripheral 3, indet. cervical vertebral, and sacral vertebra 2.

MPEF-PV 10902.—Right quadrate, left and right prootics, right dentary, and indet. shell remains.

MPEF-PV 10903.—Left quadrate.

MPEF-PV 10904.—Right bridge peripheral.

MPEF-PV 10905.—Proximal end of ?left scapula.

MPEF-PV 10906.—A left bridge peripheral and an indet. Peripheral.

MPEF-PV 10907.—Part of a left quadrate.

MPEF-PV 10908.—Fragment of a quadrate, right peripheral 1, and a caudal vertebra.

MPEF-PV 10909.—Three caudal vertebrae.

MPEF-PV 10910.—Postdentary bones.

MPEF-PV 10911.—Right and left peripherals 3.

MPEF-PV 10912.—Basioccipital.

MPEF-PV 10913.—Cervical vertebra 4.

MPEF-PV 10914.—Left quadrate, fragment of the anterior left dentary, and a centrum of cervical vertebra 4.

MPEF-PV 10915.—Proximal end of left humerus.

MPEF-PV 10916.—Left maxilla and basioccipital.

MPEF-PV 10917.—Cervical vertebra 4.

MPEF-PV 10921.—Cervical vertebra 5.

MPEF-PV 10922.—Right jugal.

MPEF-PV 10923.—Anterior part of right peripheral 1.

MPEF-PV 10924.—Squamosal.

*Methods.*—Comparisons were made with the holotype (MACN–PV CH 2017) and previously referred specimens (MACN–PV CH 2018, MEPF–PV 3975 and 3976) of *P. walshae*.

*Digitization.*—The specimens were photographed using a reflex camera EOS with a 30–90 lens. Pictures were further processed in Photoshop CS5. Figures were composed in Illustrator CC 2017. In addition to imaging, several remains were scanned

https://doi.org/10.1017/jpa.2019.11 Published online by Cambridge University Press

using a surface scanner. The 3D scan was performed by L. Mollo from the Division of Exhibitions at MPEF with an industrial Artec 3D scanner "Space Spider" model with a resolution of 0.1mm. The software Artec Studio, version 12, was used to scan and to process the images to elaborate the 3D model. The reconstruction and the positioning of the different elements was done using the software Cinema 4D, version R19 from Maxon Company. A complete list of the scanned specimens is provided in Supplementary Data 1. Skull and lower jaw remains were combined into a single file to reconstruct in 3D those structures in *P. walshae*. A PDF with the reconstructed skull and lower jaw is provided in in Supplementary Data 2.

*Phylogenetic analysis.*—For the phylogenetic analysis we used the matrix of Sterli et al. (in press) as a starting point. We made several changes to Sterli et al.'s (in press) matrix (Supplementary Data 1). We changed several characters (e.g., changed the order of states to properly order a character, divided characters), we added characters, and we excluded some characters. We also made modifications in the scoring of several taxa (Supplementary Data 1), we added information on recently described turtles (e.g., *Platychelys oberndorferi* Wagner, 1853 by Anquetin et al., 2017 and Sullivan and Joyce, 2017; *Kallokibotion bajazidi* Nopcsa, 1923 by Pérez-García and Codrea, 2017), we replaced some taxa by others (e.g., taxonomic changes; more complete or better described taxa), and we also added some taxa (Supplementary Data 1). The final matrix is formed by 106 taxa and 250 characters (Sterli and de la Fuente, in press, Supplementary Data 3 and 4). With the new remains of *P. walshae* we were able to score almost the double number of characters for this species (51 characters scored out of 245 in Sterli et al., in press, representing 20% and 95 characters out of 250 in this manuscript, representing 38%). The matrix was built in Mesquite 3.40 (Maddison and Maddison, 2018).

We conducted a cladistic analysis using TNT 1.1 (Goloboff et al., 2003, 2008). We ran a first round of tree bisection reconnection (TBR) using Traditional Search (TS) from the menu. The first round used Wagner trees as starting trees and applied TBR to those trees. We performed 1000 replicates. If the minimum length was found less than 30 times, a New Technology Search (NTS) was used. Using NTS allows using several searching algorithms at once. All the algorithms were selected (sectorial search, ratchet, drift, tree fusing) and the minimum length was set to be hit 30 times. Once we were sure that the minimum length was hit several times (30 of more of 1000 replicates), a second round of TBR was applied to all the trees in the memory. Whenever more than one most parsimonious tree was found, a strict consensus was calculated. The "pruned tree" tool of TNT was used (Trees/Comparisons/Pruned trees) with a maximum of five pruned taxa to identify wildcard taxa. With the command "nelsen// 'taxon number'", the alternate positions of the wildcard taxa were explored. Basic indexes (consistency and retention indexes) for the MPTs were calculated. Common synapomophies were calculated. Branch supports were calculated using Bremer support and Jackknife resampling (absolute frequencies and GC frequencies) with 1000 replicates.

To explore alternate position of taxa, we used constraints based on Joyce et al. (2016) and Pérez-García and Codrea (2017) (see Supplementary Data 5 for constraints). After making the constraints, the searches were performed as explained above. After having the results of the suboptimal, constrained trees, we ran a Templeton test (Templeton, 1983). This is a nonparametric test that is used to determine whether the differences between the most parsimonious trees and the suboptimal, constrained trees are statistically significative (e.g., Wilson, 2002; Carballido et al., 2011; Mannion et al., 2013; Evers and Benson, 2019). We used the script Templeton developed by Alexander N. Schmidt-Lebuhn available at https://www.anbg.gov.au/cpbr/tools/templetontest.tnt and in the Supplementary Data 6. Because the Templeton test only compares two trees, we randomly selected one of the most parsimonious trees and one of the suboptimal, constrained trees.

*Anatomical abbreviations.*—A, D, E, F, G, H, J, X, XY, Y, skull roof scutes; a, acromion; aam, area articularis mandibularis; acaf, atlas centrum articular facet; acst, aditus canalis stapedio temporalis; afi, articulation with fibula; aiaf, atlas intercentrum articular facet; ane, apertura narium externa; ati, articulation with tibia; btb, basis tuberculi basalis; ca, chevron articulation; cc, canalis cavernosus; ccc, canalis carotici cerebralis; CE, cervical scute; cl, cavum labyrinthicum; cm, condylus mandibularis; cp, coronoid process; co, condilus occipitalis; coaf, condylus occipitalis articular facet; csa, canalis semicircularis anterius; csh, canalis semicircularis horizontalis; csp, canalis semicircularis posterius; cst, canalis stapedio temporalis; ct, cavum tympani; ctm, cavum tympani margin; dip, diapophysis; dp, dorsal process of the scapula; dpp, descending process of the parietal; ecc, ectepicondylar canal; ect, ectepicondyle; ent, entopicondyle; exo, exoccipital; ica, incisura columella auris; fact, foramen anterius chorda tympani; faf, fossa acustico-facialis; fai, foramen alveolaris inferius; fic, foramen intermandibularis caudalis; fja, foramen jugulare anterius; fjp, foramen jugulare posterius; fh, femoral head; fnat, foramen nervi auriculo temporalis; fo, fenestra ovalis; fp, foramen prootic; fpct, foramen posterius chorda tympani; fr, frontal; gl, glenoid; hh, humeral head; itf, intertrochanteric fossa; lp, lateral process; lr, labial ridge; MA, marginal scute; mat, muscular attachment; mp, medial process; nec, neural crest; nc, neural canal; op, opisthotic; orn, ornamentation; orb, orbit; ow, otic wall; pa, parietal; pap, parapophysis; pi, processus interfenestralis; po, postorbital; prf, prefrontal; prz, prezygapophysis; pto, processus trochlearis oticum; pz, postzygapophysis; qu, quadrate; r-ul, radio-ulna ligament; s, suture; sbo, suture with basioccipital; sbs, suture with basisphenoid; sc, sacral centrum; scm, sulcus cartilaginis meckelii; sco, suture with coracoid; scor, suture with coronoid; sden, suture with dentary; sh, shoulder; sju, suture with jugal; smx, suture with maxilla; sna?, suture with nasal?; spmx, suture with premaxilla; sprf, suture with prefrontal; spo, suture with postorbital; sprf, suture with prefrontal; spro, suture with prootic; spt, suture with pterygoid; squ, suture with quadrate; sqj, suture with quadratojugal; sspl, suture with splenial; ssq, suture with squamosal; tma, trochanter major; tmi, trochanter minor; to, tubera occipitalis; tp, transverse process; ts,

https://doi.org/10.1017/jpa.2019.11 Published online by Cambridge University Press

triturating surface; V, vertebral scute; vcr, ventral crest; vf, vascular foramen; VII, VIII, IX, XII, cranial nerves.

*Repositories and institutional abbreviations.*—MACN–PV CH, Vertebrate Paleontology, Chubut province collection, Museo Argentino de Ciencias Naturales "Bernardino Rivadavia", Buenos Aires, Argentina; MPEF-PV, Vertebrate Paleontology, Museo Paleontológico "Egidio Feruglio", Trelew, Argentina.

## Systematic paleontology

Testudinata Klein, 1760 (sensu Joyce, Parham, and Gauthier, 2004)
Perichelydia Joyce, 2017
Meiolaniformes Sterli and de la Fuente, 2013
*Peligrochelys* Sterli and de la Fuente, 2013

*Type species.*—*Peligrochelys walshae* Sterli and de la Fuente, 2013

*Peligrochelys walshae* Sterli and de la Fuente, 2013
Figures 2–10

2013 *Peligrochelys walshae* Sterli and de la Fuente, 2013, p. 839, figs. 4–9.

*Holotype.*—MACN–PV CH 2017, several skull bones (basisphenoid, basioccipital, right quadrate, right prootic, left opisthotic, a fragment of the right opisthotic, left exoccipital, right frontal, both postorbitals, fragment of left maxilla, fragments of both squamosals and other skull roof) and a left prezygapophysis.

*Emended diagnosis.*—*Peligrochelys walshae* belongs to the clade Testudinata because it has a complete carapace and plastron enclosing the pectoral girdle. It differs from the basal members of Testudinata (taxa outside Perichelydia clade) by the reduction of the processus interfenestralis of the opisthotic, absence of the processus basitrabecularis, and an enclosed canalis cavernosus. *Peligrochelys walshae* is referred to the clade Meiolaniformes by the large exposure of the prefrontal in the skull roof, the lack of frontal contribution to the orbit, presence of protuberances in the squamosal, and formed cervical and caudal vertebrae. It is also a member of the Meiolaniformes showing the unique combination of the following characters (autapomorphies are marked with asterisks): skull roof covered by scales; presence of XY scale*; pentagonal frontal; presence of a posterior wall separating the fossa orbitalis from the fenestra temporalis inferior; jugal forming part of the triturating surface; cheek not emarginated; quadratojugal forming the anteroventral rim of the cavum tympani; presence of a processus trochlearis oticum; cavum tympani well developed; thick basicranium; presence of two concavities in the basioccipital delimited by the well-developed tubera basioccipitalis*; foramina carotici cerebralis posterior located close together; absence of a foramen posterior canalis carotici interni; foramen carotici cerebralis anterior united forming a slit*; paired pits present in the basisphenoid and developing posteriorly reaching the basioccipital; long symphysis in the dentary; only labial and lingual ridges present in dentary; no ridges in the triturating surface of the symphysis; fused postdentary bones; short processus retroarticularis; nuchal notch reaching peripheral 1; formed cervical and caudal vertebrae; differs from *Ka. bajazidi* and *Naomichelys speciosa* Hay, 1908 because of anterior caudal vertebrae are opisthocoelous and the posterior caudal vertebrae are procoelous, and due to the shape of the basioccipital. It can be distinguished from *Patagoniaemys gasparinae* Sterli and de la Fuente, 2011b, *Mongolochelys efremovi* Khosatzky, 1997, *Chubutemys copelloi* Gaffney et al., 2007, and *Niolamia argentina*, Ameghino, 1899 by the presence of a short anterior process of postorbital forming the posteriormost margin of the orbit. *Peligrochelys walshae* shares with *Pa. gasparinae* and *Mo. efremovi* the presence of a wide and short, trapezoidal nuchal.

*Occurrence.*—Several sites in the vicinity of the Punta Peligro locality (Fig. 1), Chubut Province, Argentina. Banco Negro Inferior level of the Salamanca Formation (Lesta and Ferrello, 1972), Danian (lower Paleocene) (Clyde et al., 2014). For more information about the Salamanca Formation see Sterli and de la Fuente (2013).

*Materials.*—MACN–PV CH 2018 and MPEF-PV 3975 and 3976. MPEF-PV 10831–10839, 10902–19017, and 10921–10924.

*Remarks.*—Many cranial and postcranial materials of additional specimens referred to *P. walshae*, here described, allow us to expand the diagnosis of this species, previously only known by cranial remains represented by the holotype and three referred specimens.

## Description

*Skull morphology.*—Using the 3D reconstruction of the skull (based on several specimens), we estimate that the length of the skull was ~9.5 cm and the width was 13 cm. Skull remains are described in the following paragraphs and are illustrated in Figures 2–4.

*Scales.*—The dermal bones of *P. walshae* were covered with scales. Scales are recognized in specimens MPEF-PV 10831, 10832–10834, and 10913. Paired scales D, E, F1, F2, F3, F4, G, H, J1, J2, and J3 and uneven scales A, X, Y, XY, and Z are recognized (Figs. 2.1, 2.3, 2.4, 2.6, 3.3).

Regarding paired scales, part of scale D (MPEF-PV 10832) is preserved on the parietal. Its preserved contacts are the anteromedial with scale X and the posteromedial with scale A. Part of scale E is preserved on the jugal (MPEF-PV 10833). It contacted scales J1 anteriorly and J3 ventrally. More details are not apparent. Scale F1 (MPEF-PV 10832) covers mainly the postorbital and a small piece of the frontal. It contacts scale F4 anteriorly, Y medially, G posteromedially, H posteriorly, F3 laterally, and a small part of F2 posterolaterally. Scale F2 (MPEF-PV 10832) is located on the postorbital. It contacts F3 anteriorly, H medially, and a small part of F1

https://doi.org/10.1017/jpa.2019.11 Published online by Cambridge University Press

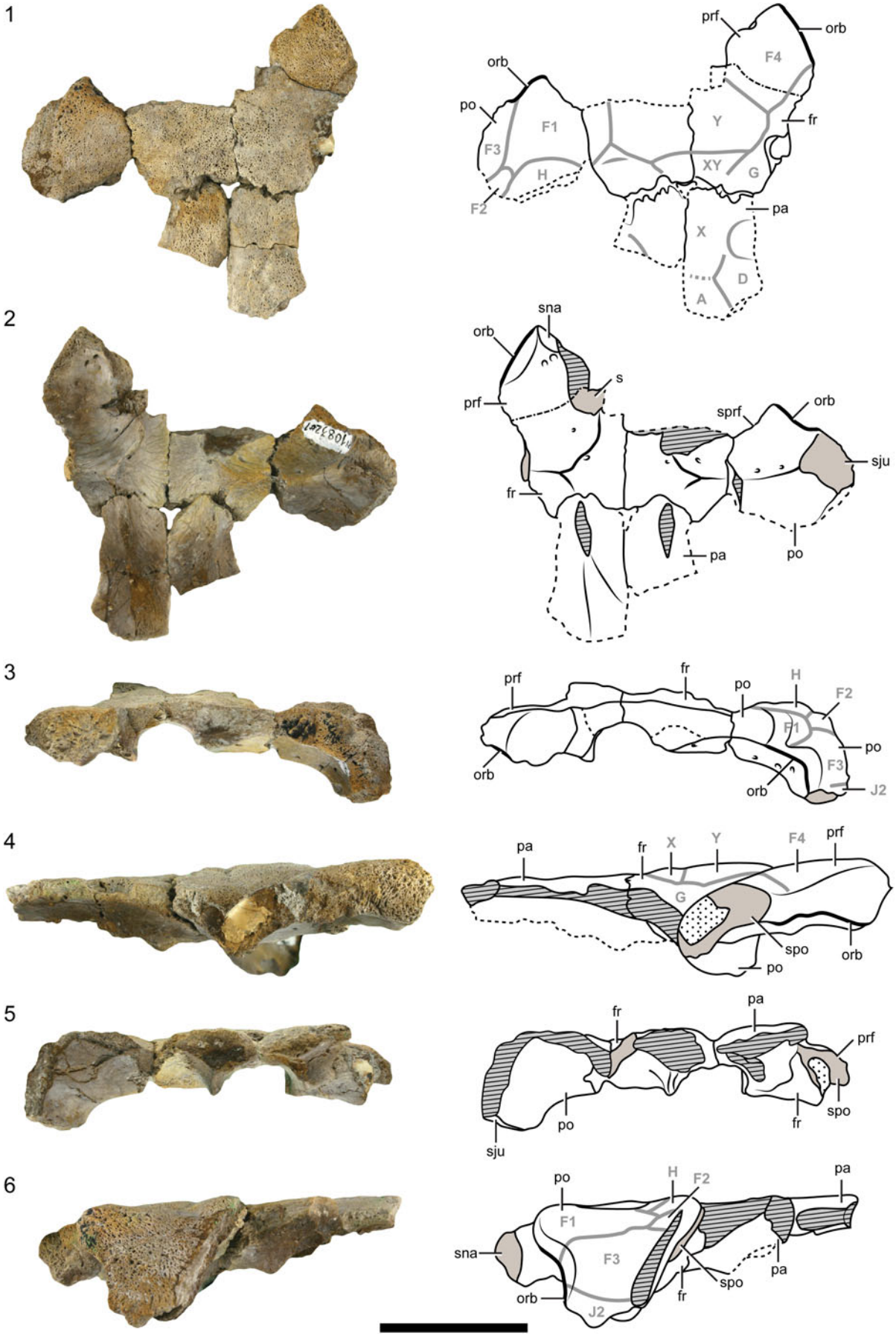


https://doi.org/10.1017/jpa.2019.11 Published online by Cambridge University Press

**Figure 2.** *Peligrochelys walshae* from the Salamanca Formation, Danian, Chubut Province, Argentina. Pictures and drawings of the skull roof MPEF-PV 10832 in (**1**) dorsal view; (**2**) ventral view; (**3**) anterior view; (**4**) right lateral view; (**5**) posterior view; (**6**) left lateral view. Black, continuous lines indicate natural borders and sutures. Black, dashed lines indicate broken edges. Gray thick lines indicate scute sulci. Diagonal pattern indicate broken bone. Spotted pattern indicates sediment. Scale bar represents 5 cm. Abbreviations: A, D, F, G, H, J, X, XY, Y, skull roof scutes; fr, frontal; orb, orbit; pa, parietal; po, postorbital; prf, prefrontal; s, suture; sju, suture with jugal; sna, suture with nasal; spo, suture with postorbital; sprf, suture with prefrontal.

anterolaterally. No other contacts of F2 are preserved. Scale F3 (MPEF-PV 10832) is a small scale surrounded by F1 dorsally, F2 posteriorly, and J2 ventrally. Scale F4 is situated on the prefrontal and frontal (MPEF-PV 10832). It contacts F1 posterolaterally and Y posteromedially. The remaining contacts are not preserved. Only the anteriormost part of scale G is preserved on the frontal (MPEF-PV 10832). This scale contacts scale Y anteriorly, F1 anterolaterally, H laterally, and XY scale medially. The remaining contacts are not preserved. Scale H is preserved on the postorbital (MPEF-PV 10832). The preserved contacts of scale H are with F1 anteriorly, G medially, and F2 laterally. A small remain of scale J1 is preserved on the jugal (MPEF-PV 10833). It contacts scale E posterodorsally and J3 posteriorly. Other contacts are not preserved. Also a small remain of scale J2 is preserved on the ventral part of postorbital (MPEF-PV 10832). Only the contact with F3 is preserved. Scales F1, F3, F4, and J2 form part of the orbital rim. Scale J3 is preserved in the posteroventral part of jugal (MPEF-PV 10833). Its preserved contacts are with scale E dorsally and scale J1 anteriorly.

Regarding unpaired scales, a small fragment of scale A is preserved on the parietal (MPEF-PV 10832). The preserved contacts are with scale X anteriorly and D anterolaterally. Scale X is preserved almost complete on the parietal (MPEF-PV 10832). Its preserved contacts are with scales XY anteriorly, G anterolaterally, A posteriorly, and D posterolaterally. A remain of scale Z is located in the anteromedial part of the frontals (MPEF-PV 10831). The preserved contacts are posteriorly with scale Y and laterally with scale F4. A new scale (we called it XY because it is located between scales X and Y) is preserved in specimen MPEF-PV 10832. It is a small scale, triangular, located along the midline. It contacts scale Y anteriorly, X posteriorly, and scale G laterally. Scale Y is the biggest preserved scale and covers the frontal (MPEF-PV 10832). It contacts scale Z anteriorly, F4 anterolaterally, F1 laterally, and G posteriorly.

In addition of being covered by scales, the dermal bones exhibit an ornamentation formed by several small ridges and small pits randomly arranged. The small pits are also present in the holotype, but not the ridges. This could be caused by erosion of the bone or as a result of ontogenetic changes. This decoration is very different from that recognized in the Helochelydridae *Naomichelys speciosa*, where the entire skull roof is covered with low tubercles (Joyce et al., 2014, fig. 3).

*Dermal roofing.*—The preserved dermal roofing elements of this species are the prefrontal, frontal, parietal, jugal, quadratojugal, squamosal, and postorbital.

A complete, right prefrontal is preserved in MPEF-PV 10832 (Fig. 2.1–2.4). It is a triangular, thick element that forms part of the skull roof and the orbital margin. It contacts the frontal posteromedially and the anterior contact with the nasal and the posterolateral contact with the postorbital are suggested.

The frontal bone is illustrated in Figure 2.1–2.5. There are three new frontals, one right frontal (MPEF-PV 10831), and one right and one left frontal (MPEF-PV 10832). The general shape and structures of the preserved frontals are similar to those present in the holotype, although there are some differences. The frontal from the holotype (MACN–PV CH 2017) has five well-defined sides, while the frontals of MPEF-PV 10831 and 10832 have four well-developed sides and a very small fifth side. The outline of this bone is roughly triangular in *Chubutemys copelloi* (Sterli et al., 2015a, figs. 2, 3), in *Mongolochelys efremovi* (Sukhanov, 2000, fig. 17.28; Danilov et al., 2017, fig.10), and in *Meiolania platyceps* Owen, 1886 (Gaffney, 1983, fig. 21). In *Kallokibotion bajazidi*, the shape of the frontal is variable, as well as its contribution to the orbital margin (Pérez-García and Codrea, 2017). Although both frontals in *P. walshae* are thick elements, the frontal of the holotype is much thicker than the ones from the new specimens. These listed differences might be related with changes through ontogeny, because their sizes are slightly different. The frontal has sutural surfaces with the parietal posteriorly, the postorbital laterally, with the prefrontal anteriorly, and the other frontal medially. The shape of the frontal suggests that the frontal separated the posterior part of the prefrontals. The frontal did not form part of the orbital rim (as also shown by the other specimens), as in *Chubutemys copelloi* (Gaffney et al., 2007, figs. 4, 5; Sterli et al., 2015a, figs 2, 3), *Mongolochelys efremovi* (Sukhanov, 2000, fig. 17.28; Danilov et al., 2017, fig.10), *Meiolania platyceps* (Gaffney, 1983, fig. 21), *Niolamia argentina* (Sterli and de la Fuente, 2011a, fig. 1), and some specimens of *K. bajazidi* (Pérez-García and Codrea, 2017). To the contrary, a minor participation of the frontal in the orbital rim is seen in some specimens of *Kallokibotion bajazidi* (Pérez-García and Codrea, 2017). Also, as in the other known specimens of *P. walshae*, in ventral view the frontal forms the roof of the fossa orbitalis (laterally), the sulcus olfactorius (medially), and part of the fossa nasalis (anteriorly).

The anteromedial part of both parietals is preserved in specimen MPEF-PV 10832 (Fig. 2.1, 2.2, 2.4–2.6). The parietal forms part of the skull roof. The only preserved contacts are the anterior one with the frontal and the medial one with its counterpart. Ventrally the parietal has the descending process that encloses the endocranial cavity.

Three right jugals are known from *P. walshae* (MPEF-PV 10832, 10833, and 10922). It is a tall bone, taller than wide (Fig. 3.1, 3.2). A tall bone is also recognized in *Chubutemys copelloi* (Sterli et al., 2015a). In *Peligrochelys walshae*, the jugal bears sutural surfaces with the postorbital dorsally, the maxilla anteriorly, and the quadratojugal posteriorly (Fig. 2.2). It forms a small part of the posteroventral rim of

https://doi.org/10.1017/jpa.2019.11 Published online by Cambridge University Press

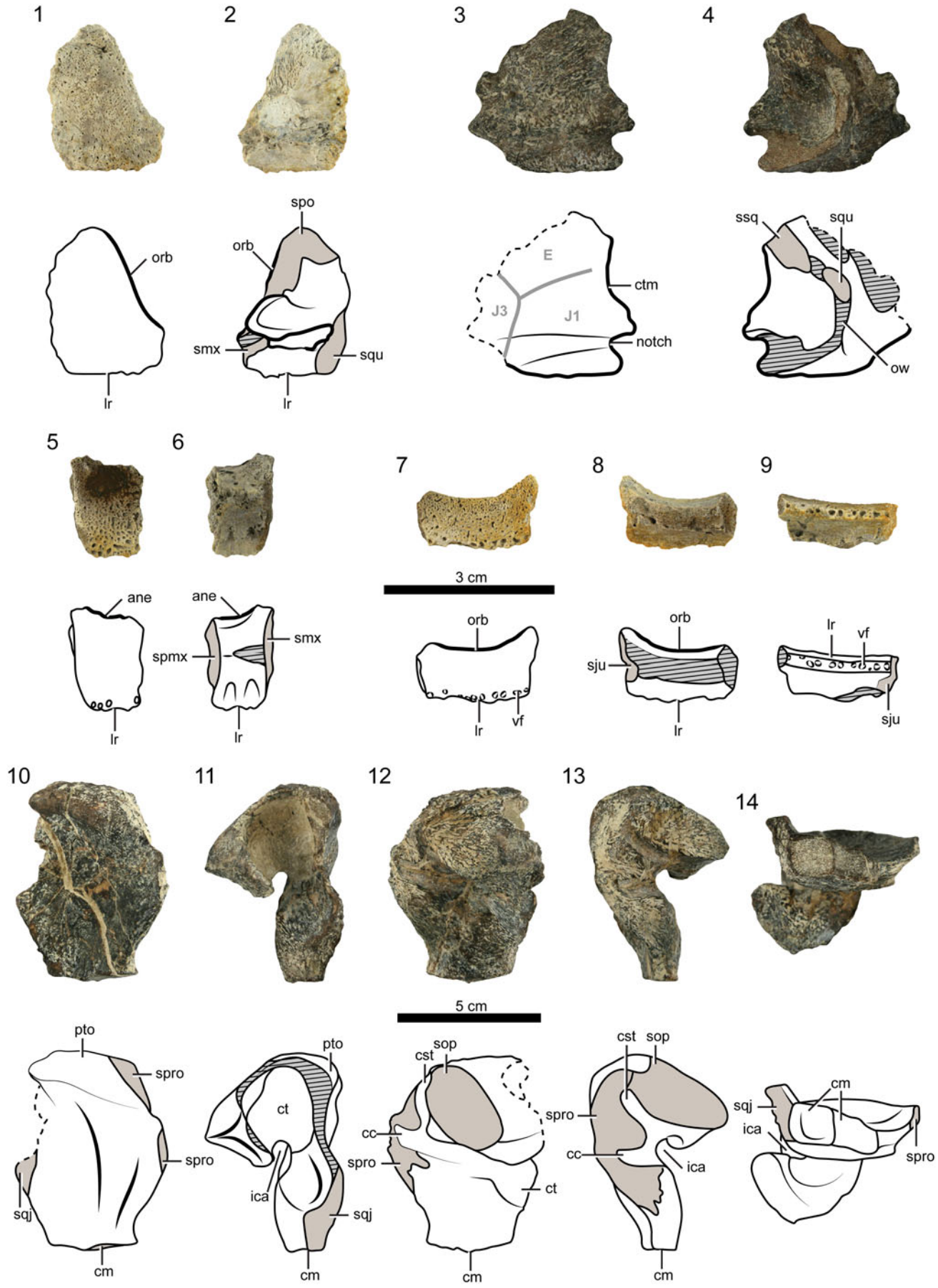


https://doi.org/10.1017/jpa.2019.11 Published online by Cambridge University Press

**Figure 3.** *Peligrochelys walshae* from the Salamanca Formation, Danian, Chubut province, Argentina. Pictures and drawings of (**1**) skull remains of right jugal (MPEF-PV 10833) in right lateral view; (**2**) right jugal in medial view; (**3**) left quadratojugal (MPEF-PV 10831) in left lateral view; (**4**) left quadratojugal in medial view; (**5**) right premaxilla (MPEF-PV 10832) in anterior view; (**6**) right premaxilla in posterior view; (**7**) left maxilla (MPEF-PV 10916) in left lateral view; (**8**) left maxilla in medial view; (**9**) left maxilla in ventral view; (**10–14**) right quadrate (MPEF-PV 10831) (**10**) in anterior view; (**11**) in right lateral view; (**12**) in posterior view; (**13**) in medial view; (**14**) in ventral view. Scale bars represent 3 cm in (**1–9**), 5 cm in (**10–14**). Abbreviations: ane, apertura narium externa; cc, canalis cavernosus; cm, condylus mandibularis; cst, canalis stapedio temporalis; ct, cavum tympani; ctm, cavum tympani margin; E, J1, J3, skull roof scutes; ica, incisura columella auris; lr, labial ridge; orb, orbit; ow, otic wall; pto, processus trochlearis oticum; sju, suture with jugal; smx, suture with maxilla; sop, suture with opisthotic; spmx, suture with premaxilla; spo, suture with postorbital; spro, suture with prootic; sqj, suture with quadratojugal; squ, suture with quadrate; ssq, suture with squamosal; vf, vascular foramen.

the orbit and posteriormost part of the triturating surface (Fig. 3.2). Only the labial ridge of the triturating surface can be observed.

A big portion of the left quadratojugal is preserved in specimen MPEF-PV 10831 (Fig. 3.3, 3.4). The only preserved sutural area is the dorsal one, presumably with the squamosal. The quadratojugal might have also contacted the postorbital anterodorsally and the quadrate posteriorly. A contact quadratojugal-jugal that prevents the quadratojugal-maxilla contact is also present in *Chubutemys copelloi* and in *Meiolania platyceps* (Gaffney, 1983; Gaffney et al., 2007; Sterli et al., 2015a). Two different reconstructions are illustrated for *Mongolochelys efremovi*: Suzuki and Chinzorig (2010, fig. 1) show a sutural contact between maxilla and quadratojugal, whereas Sukhanov (2000, fig. 17.28) and Danilov et al. (2017, fig. 10) illustrated only a maxilla-jugal contact. The quadratojugal forms the border for the cheek, suggesting it was not emarginated. The quadratojugal also forms the anteroventral part of the external rim of the cavum tympani. In the ventral part of the quadratojugal, there is a trough and ventral to it the rim of the cheek is seen. In medial view there is a process that might contact the anterior part of the quadrate.

There is a fragment of squamosal with a knob in specimen MPEF-PV 10924, which has also been found in the holotype.

The postorbital bone is illustrated in Figure 2.1–2.6. Two left (MPEF-PV 10831 and 10832) and two right postorbitals (MPEF-PV 10831 and 10834) are preserved. The postorbital bears the sutural surfaces for the prefrontal and frontal anteromedially, the parietal posteromedially, and the jugal ventrally. As it is seen in the holotype, the postorbital forms part of the skull roof, the posterodorsal rim of the orbit, and part of the roof of the fossa orbitalis. In *P. walshae*, the anterior process of the postorbital is short and forms the posteriormost margin of the orbit, as in *Kallokibotion bajazidi* (Gaffney and Meylan, 1992, figs. 1–6; Pérez-García and Codrea, 2017, fig. 2). Conversely, in *Pa. gasparinae* (Sterli and de la Fuente, 2011b, fig. 3), in *Mongolochelys efremovi* (Sukhanov, 2000, fig. 17.28; Suzuki and Chinzorig, 2010, fig. 1), in *Niolamia argentina* (Sterli and de la Fuente, 2011a, figs. 1, 3), and in *Chubutemys copelloi* (Sterli et al., 2015a, figs. 2, 3), the postorbital has an extensive anterior process. In *P. walshae*, as in *M. efremovi*, *Meiolania platyceps*, and *Niolamia argentina*, the postorbital is much more robust than in *Pa. gasparinae*.

*Palatal elements.*—New palatal elements in *P. walshae* include the premaxilla and maxilla. The right premaxilla is preserved in specimen MPEF-PV 10832 (Fig. 3.5, 3.6). It is a small element. The preserved contact surfaces are with the maxilla laterally, the other premaxilla medially, and probably with the nasal laterodorsally. Dorsally, it formed the ventral rim of the apertura narium externa and ventrally the anterior end of the triturating surface.

The posterior part of the left maxilla is preserved in specimen MPEF-PV 10916 (Fig. 3.7–3.9). Posteriorly the sutural surface with the jugal is preserved. Dorsally it forms the ventral part of the orbital rim and ventrally it forms part of the triturating surface. Only the labial ridge is preserved.

*Palatoquadrate elements.*—The quadrate is the only preserved bone derived from the palatoquadrate element. The quadrate bone is illustrated in Figure 3.10–3.14. There are six left quadrates (MPEF-PV 10831, 10914, 10832, 10833, 10903, 10907) and three right quadrates (MPEF-PV 10831, 10832, 10902). The general shape of the quadrate is similar to the one described for the holotype. The quadrate shows the articulation surfaces for the quadratojugal (anteriorly), prootic and pterygoid (medially), for the jugal (laterally), for the opisthotic (posteriorly), and for the squamosal posterodorsally. The quadrate might have contacted the squamosal, but the articulation surface for this bone is not preserved. It has a deep cavum tympani and the incisura columella auris is open posteriorly, at least in the path of the quadrate. Anterodorsally, the quadrate bears a processus trochlearis oticum. Ventrally, it bears the articular process that in turns bears at the most ventral end the condylus mandibularis. The condyle has two articular surfaces delimited by a short, anteroposteriorly directed ridge. The medial part of the condyle is almost flat, wider than long, while the lateral part is slightly concave, quadrangular in outline. In medial view, the aditus canalis stapedio temporalis and the canalis cavernosus are visible. There is a small passage connecting both canals (the name or function of this canal is unknown).

*Braincase elements.*—The exoccipital, basioccipital, prootic, opisthotic, and basisphenoid are the new elements known from the braincase. The exoccipital bone is illustrated in Figure 4.1–4.3. Two left exoccipitals are preserved (MPEF-PV 10831, 10832) and one right (MPEF-PV 10831). The exoccipital bears the sutural surfaces with the basioccipital (ventrally) and the opisthotic (laterally). The suture with the supraoccipital is not preserved. The exoccipital forms the lateral rim of the foramen magnum. Two foramen nervi hypoglossi are preserved in the exoccipital. This is a difference with the holotype in which both foramina are confluent. The exoccipital, together with the opisthotic, forms part of the foramina jugulare anterius and posterius. The foramen jugulare posterius is coalescent with the fenestra postotica as in

https://doi.org/10.1017/jpa.2019.11 Published online by Cambridge University Press

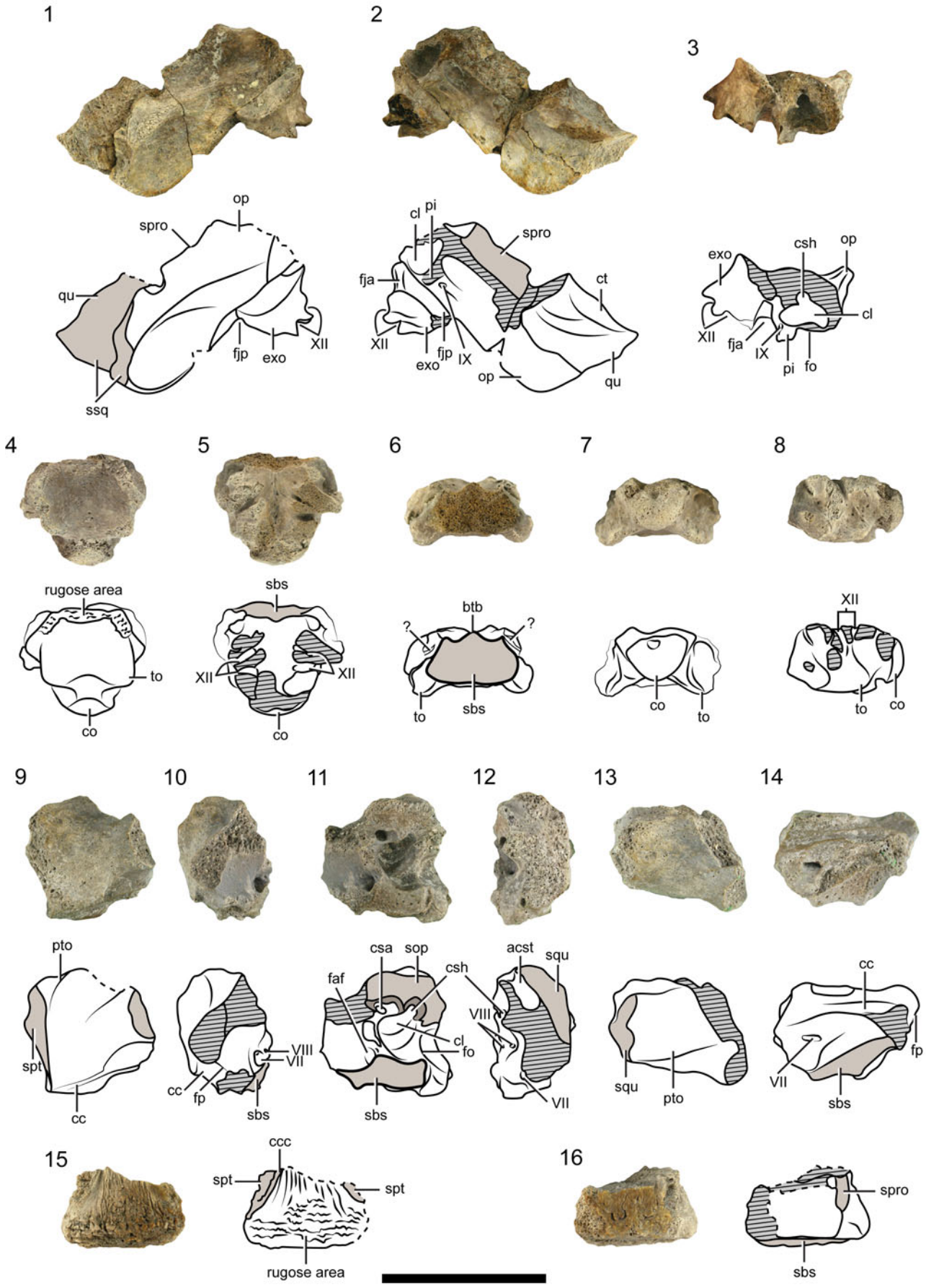


https://doi.org/10.1017/jpa.2019.11 Published online by Cambridge University Press

**Figure 4.** *Peligrochelys walshae* from the Salamanca Formation, Danian, Chubut Province, Argentina. Pictures and drawings of skull remains of left opisthotic, left exoccipital, and a fragment of the left quadrate (MPEF-PV 10832) in (**1**) posterior view; (**2**) ventral view; (**3**) medial view; basioccipital (MPEF-PV 10916) in (**4**) ventral view; (**5**) dorsal view; (**6**) anterior view; (**7**) posterior view; (**8**) left lateral view; prootic (MPEF-PV 10902) in (**9**) anterior view; (**10**) anteromedial view; (**11**) medial view; (**12**) posterior view; (**13**) dorsal view; (**14**) ventral view; basisphenoid (MPEF-PV 10833) in (**15**) ventral view; (**16**) dorsal view. Black, continuous lines indicate natural borders and sutures. Black, dashed lines indicate broken edges. Gray thick lines indicate scute sulci. Diagonal pattern indicates broken bone. Scale bar represents 3 cm. Abbreviations: acst, aditus canalis stapedio temporalis; btb, basis tuberculi basalis; cl, cavum labyrinthicum; cc, canalis cavernosus; ccc, canalis carotici cerebralis; co, condilus occipitalis; csa, canalis semicircularis anterius; csh, canalis semicircularis horizontalis; ct, cavum tympani; exo, exoccipital; faf, fossa acustico-facialis; fja, foramen jugulare anterius; fjp, foramen jugulare posterius; fo, fenestra ovalis; fp, foramen prootic; op, opisthotic; pi, processus interfenestralis; pto, processus trochlearis oticum; qu, quadrate; sbs, suture with basisphenoid; sop, sutures with opisthotic; spro, suture with prootic; spt, suture with pterygoid; squ, suture with quadrate; ssq, suture with squamosal; to, tubera occipitalis; VII, VIII, IX, XII, cranial nerves.

*Kallokibotion bajazidi*, *Ch. copelloi*, *Me. Platyceps*, and *Mongolochelys efremovi*. Posteriorly, the exoccipital possesses a crest, maybe related with muscle attachment.

The basioccipital bone is illustrated in Figure 4.4–4.8. Two basioccipitals (MPEF-PV 10912 and 10916) are preserved. It is a thick bone. In ventral view, a pair of tubera basioccipitalis is visible, as in other meiolaniforms. A concavity is recognized between both tubera, as in *K. bajazidi*, *M. efremovi*, and meiolaniids. Contrary to the holotype of *Peligrochelys walshae*, the concavity in this specimen is not divided in the midline by a low ridge that bifurcates posteriorly. However, it is interesting to note that both new basioccipitals are much smaller than in the holotype. The occipital condyle is sub-triangular to triangular in outline and slightly wider than high, and it is separated from the main body of the basioccipital by a short neck, as in the holotype of *P. walshae*. Because the sutures between the basioccipital and exoccipitals cannot be recognized, as well as the participation of the exoccipitals in the condyle, we presume those bones are fused.

The prootic bone is illustrated in Figure 4.9–4.14. One left (MPEF-PV 10902) and two right (MPEF-PV 10832 and 10902) prootics are preserved. The general morphology of the prootic is similar to the holotype of *P. walshae* (Sterli and de la Fuente, 2013, figs. 6, 7). The prootic preserves the sutural surfaces with the quadrate (laterally), with the pterygoid and basisphenoid (ventrally), opisthotic (posteriorly), and parietal (dorsally). In anterior view, the processus trochlearis oticum, the canalis cavernosus, and the prootic foramen are visible. In medial view, the wall of the cavum cranii, the fossa acustico-facialis pierced by the foramen nervi facialis (VII) and by two foramina nervi acustici (VIII), the anterior rim of the hiatus acusticus, and the canalis semicircularis anterius and horizontalis are observed. In posterior view, the cavum labyrinthicum, the recessus labyrinthicus prooticus, the canalis semicircularis horizontalis and the anterior rim of the fenestra ovalis are seen. In lateral view, the medial border of the aditus canalis stapedio-temporalis is recognized. In ventral view, the prootic is pierced by the facial nerve (VII). The anteroventral part of the prootic forms the posterior wall of the canalis cavernosus. In medial and posterior view, the inner ear is seen delimited by the fenestra ovalis and containing the recessus labyrinthicus prooticus. In the medial wall, the foramen nervi facialis (VII) and two foramina nervi acustici (VIII) are preserved.

The left opisthotic and some small fragments of the right one are preserved in specimen MPEF-PV 10832 (Fig. 4.1–4.3). The opisthotic is similar to the one preserved in the holotype (Sterli and de la Fuente, 2013, figs. 8, 9). The preserved contacts are with the exoccipital posteromedially and the quadrate anterolaterally. In the dorsolateral corner, there is a sutural surface presumably for the squamosal. The opisthotic likely contacted the prootic anteromedially and the supraoccipital dorsoanteriorly. In posterior view, the opisthotic has a horizontal crest, as is also seen in the holotype. This crest could be related to muscle attachment. The opisthotic forms part of the recessus labyrinthicus opisthoticus. The processus interfenestralis of the opisthotic is a delicate strip of bone pierced by the foramina for the nervi glossopharyngei (IX). Posterior to the processus interfenestralis, the recessus scalae tympani is preserved. Through this space the vagus (X) and accessory (XI) nerves and the vena capitis cerebralis leave the skull (Gaffney, 1979). This recessus opens to the exterior through the foramen jugulare posterius (maybe formed by the exoccipital and opisthotic in *P. walshae*). The foramen jugulare anterius connects the recessus scalae tympani with the cavum cranii (Gaffney, 1979) and it is formed by the opisthotic and the exoccipital in *P. walshae*.

The posterior part of the basisphenoid is preserved in specimen MPEF-PV 10833 (Fig. 4.15, 4.16). The basisphenoid is similar to the one present in the holotype (Sterli and de la Fuente, 2013, figs. 8, 9). Although it is an isolated element, the sutural surface with the basioccipital posteriorly, with the pterygoid mediolaterally, and with the prootic dorsomedially are preserved. It is a thick element. In ventral view, near the suture with the basioccipital, a wrinkled area is seen. The sulcus leading to the foramen caroticus cerebralis posterius is seen in ventral view. As it is seen in the holotype of *Pe. walshae* (MACN PV CH 2017), the basisphenoid is roughly triangular in shape and its basis is as wide as the basioccipital (Sterli and de la Fuente, 2013, fig. 8). In contrast, in *Naomichelys speciosa*, the parabasisphenoid is bottle-shaped, and the basis of this bone is narrower than the basioccipital (Joyce et al., 2014, fig. 2).

*Lower jaw.*—The lower jaw of *P. walshae*, as in all turtles, is represented by the dentary and postdentary bones. In *Peligochelys walshae*, as in other meiolaniforms, a web of bone connects both dentaries behind and below the symphysis, the triturating surfaces are relatively narrow, and the fossa meckelii is not obscured by the processus coronoideus. To the contrary, in *Naomichelys speciosa*, a broad shelf is developed along the symphysis, the triturating surfaces are extremely broad and low, and the coronoid process is folded medially making the mandible of this species highly unusual in general morphology (Joyce et al., 2014, fig. 5).

*Dentary.*—The dentary bone is illustrated in Figure 5.1–5.6. One right (MPEF-PV 10902), two symphyses (MPEF-PV

https://doi.org/10.1017/jpa.2019.11 Published online by Cambridge University Press

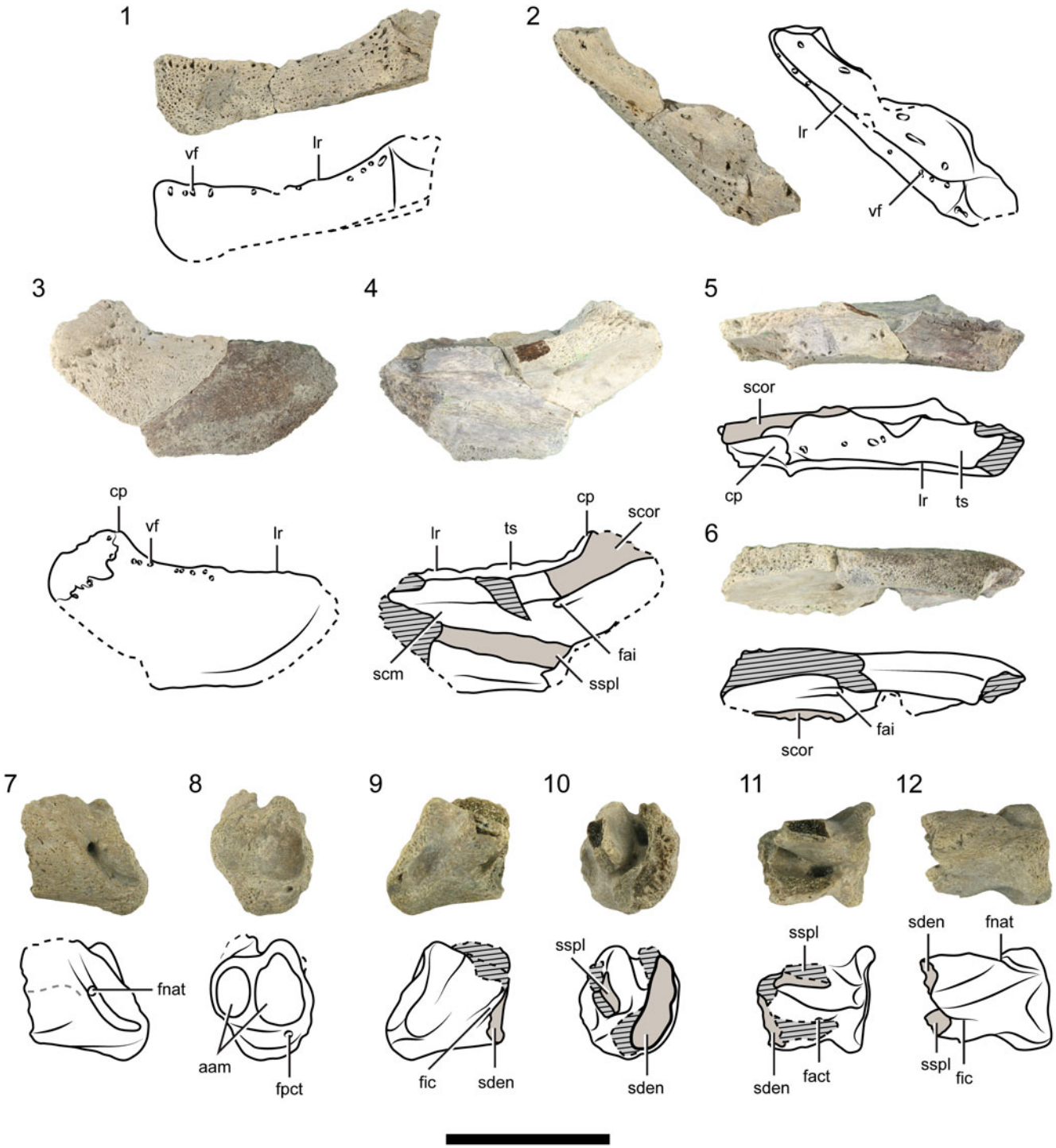


**Figure 5.** *Peligrochelys walshae* from the Salamanca Formation, Danian, Chubut province, Argentina. Pictures and drawings of left dentary of lower jaw (MPEF-PV 10832) in (**1**) left lateral view; (**2**) dorsal view; right dentary (MPEF-PV 10902) in (**3**) lateral view; (**4**) medial view; (**5**) dorsal view; (**6**) ventral view; left post-dentary bones (MPEF-PV 10910) in (**7**) lateral view; (**8**) posterior view; (**9**) medial view; (**10**) anterior view; (**11**) dorsal view; (**12**) ventral view. Black, continuous lines, natural borders and sutures. Black, dashed lines, broken edges. Diagonal pattern, broken bone. Spotted pattern, sediment. Scale bar represents 3 cm. Abbreviations: aam, area articularis mandibularis; cp, coronoid process; fact, foramen anterius chorda tympani; fai, foramen alveolaris inferius; fic, foramen intermandibularis caudalis; fnat, foramen nervi auriculo temporalis; fpct, foramen posterius chorda tympani; lr, labial ridge; scm, sulcus cartilaginis meckelii; scor, suture with coronoid; sden, suture with dentary; sspl, suture with splenial; ts, triturating surface; vf, vascular foramen.

10838 and 10914), and two left (MPEF-PV 10832 and 10914) dentaries are preserved. Externally, the dentary shows ornamentation as the one present in the dermal bones of the skull plus the presence of bigger pits near the triturating surface. These bigger pits are interpreted as nutritional foramina related with the presence of a ramphotheca. The preserved sutural areas are the posteromedial one with the coronoid, splenial, and/or with the prearticular and the

https://doi.org/10.1017/jpa.2019.11 Published online by Cambridge University Press

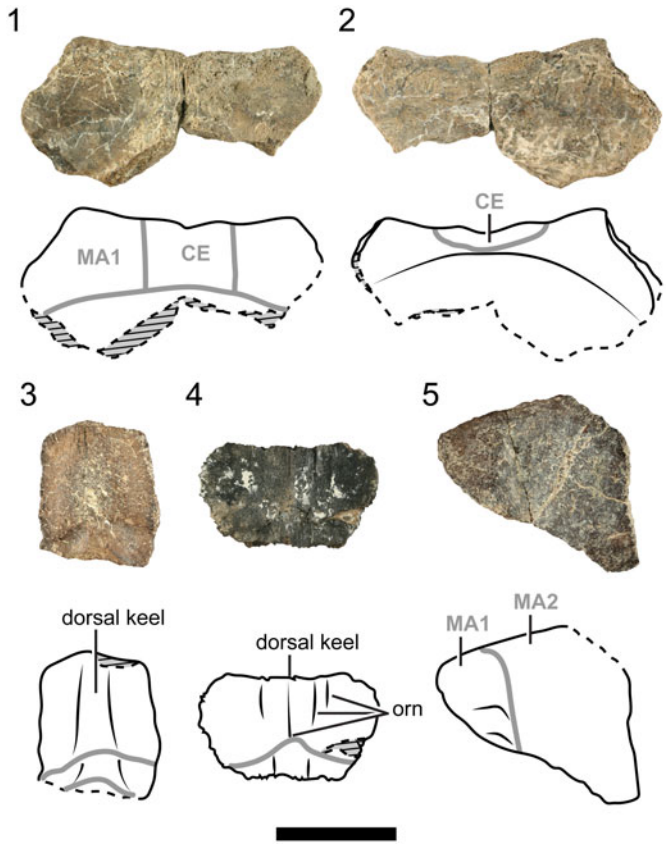


**Figure 6.** *Peligrochelys walshae* from the Salamanca Formation, Danian, Chubut Province, Argentina. Pictures and drawings of nuchal (MPEF-PV 10834) in (**1**) dorsal view; (**2**) visceral view; (**3**) neural indet. (MPEF-PV 10831) in dorsal view; (**4**) neural indet. (MPEF-PV 10833) in dorsal view; (**5**) peripheral 1 (MPEF-PV 10831) in dorsal view. Black, dashed lines indicate broken edges. Diagonal pattern indicates broken bone. Spotted pattern indicates sediment. Scale bar represents 3 cm. Abbreviations: CE, cervical scute; MA, marginal scute; orn, ornamentation.

anteromedial one with the other dentary. Both rami are fused in a relatively long symphysis. In medial view, the sulcus cartilaginis Meckelii is seen. Also in medial view, there is a foramen whose canal runs inside the dentary and at the same level as the sulcus cartilaginis Meckelii. There is no apparent anterior opening of this canal. The triturating surface is formed entirely by the dentary. In dorsal view, the triturating surface is concave, limited by the labial and lingual ridges. The labial ridge is taller anteriorly, but they are similar in height posteriorly. However, in meiolaniids, such as *Niolamia argentina* (Sterli and de la Fuente, 2011a, fig. 4, C–J) or *Meiolania platyceps*, the lingual ridge is taller than the labial one (Gaffney, 1983, figs. 61, 62), and the triturating surface is wider towards the posterior. The triturating surface is also pierced by big foramina. *Peligrochelys walshae* does not have the ridge in the symphysis or the perpendicular ridges present near the symphysis seen in *Mo. efremovi*. The coronoid process is present in the posterodorsal part of the dentary. The foramen alveolare inferius pierces the dentary in medial view below the coronoid process. In the posterior end of the dentary, there is a ridge interpreted as the posterior limit of the ramphotheca.

*Postdentary bones.*—Postdentary bones of the left ramus of lower jaw attributed to *P. walshae* is recognized in specimen MPEF-PV 10910 (Fig. 5.7–5.12). All the bones are fused, so the sutures among them are not distinguishable. We assume that the articular, surangular, angular, and prearticular bones are present. The surangular bears anteriorly the sutural area with the dentary. The surangular has the meiolaniform ornamentation with small pits randomly arranged. The foramen nervi auriculotemporalis (V3) is located well posteriorly in the surangular. The canal containing the auriculotemporal nerve runs inside the bone and opened in the fossa Meckelii. Posteroventrally to the foramen there is a groove. The area articularis mandibularis is more or less rounded in outline, concave, and is subdivided in two subequal areas by a ridge. The medial concavity is bigger than the lateral one, as in other meiolaniforms such as *Meiolania platyceps* (Gaffney, 1983, figs. 62, 63). Posterior to the area articularis mandibularis, there is a short processus retroarticularis in *P. walshae*. Conversely to the condition seen in meiolaniforms, such as *Meiolania platyceps* (Gaffney, 1983) and *Kallokibotion bajazidi* (Gaffney and Meylan, 1992). This process is pierced by the foramen chorda tympani mandibularis (VII) in *P. walshae*. The corda tympani mandibularis nerve is surrounded by bone in *P. walshae*. In medial view, a portion of the prearticular is preserved. It formed part of the rim of the foramen intermandibularis caudalis (V3).

*Carapace.*—All the carapace remains have the same ornamentation present in other meiolaniforms composed of small pits randomly oriented. The thickness of the carapacial bones differs according to each type of plate. In general, the thickness increases toward the periphery of the carapace. Neural bones are 2–3 mm thick, while the peipherals are ~4 mm thick. A different ornamentation is recognized in *Naomichelys speciosa*. In this helochelydrid species, the entire dorsal surface of the carapace is covered with pustules (Joyce et al., 2014, fig. 7).

*Nuchal (Fig. 6.1, 6.2).*—There are seven nuchals or fragments of nuchals preserved (MPEF-PV 10831, 10834–10839). The anterior border is slightly concave, but in the middle (where the cervical scute is) it has an anterior process. In contrast, the anterior margin in *Naomichelys speciosa* is characterized by a deep nuchal notch that is formed also by the peripheral 1 (Joyce et al., 2014). This large notch produces in this helochelydrid species a trapezoidal nuchal bone three times wider posteriorly than anteriorly; displaying a different outline than the shape recognized in the nuchal of *Peligrochelys walshae*. The sutural area with the peripheral 1 is preserved. Some of the outlines of the cervical, marginal 1, and vertebral 1 are recognized on the nuchal. The cervical is rectangular, slightly wider than long. The general shape of the nuchal is arched. Conversely to *Ka. bajazidi* and *Meio. platyceps*, a strong nuchal notch is recognized in *Pa. gasparinae*, *Mo. efremovi*, and likely in *P. walshae*. We infer the presence of a strong nuchal notch in *P. walshae* based on the shape of the nuchal and its articulation with the first peripheral.

https://doi.org/10.1017/jpa.2019.11 Published online by Cambridge University Press

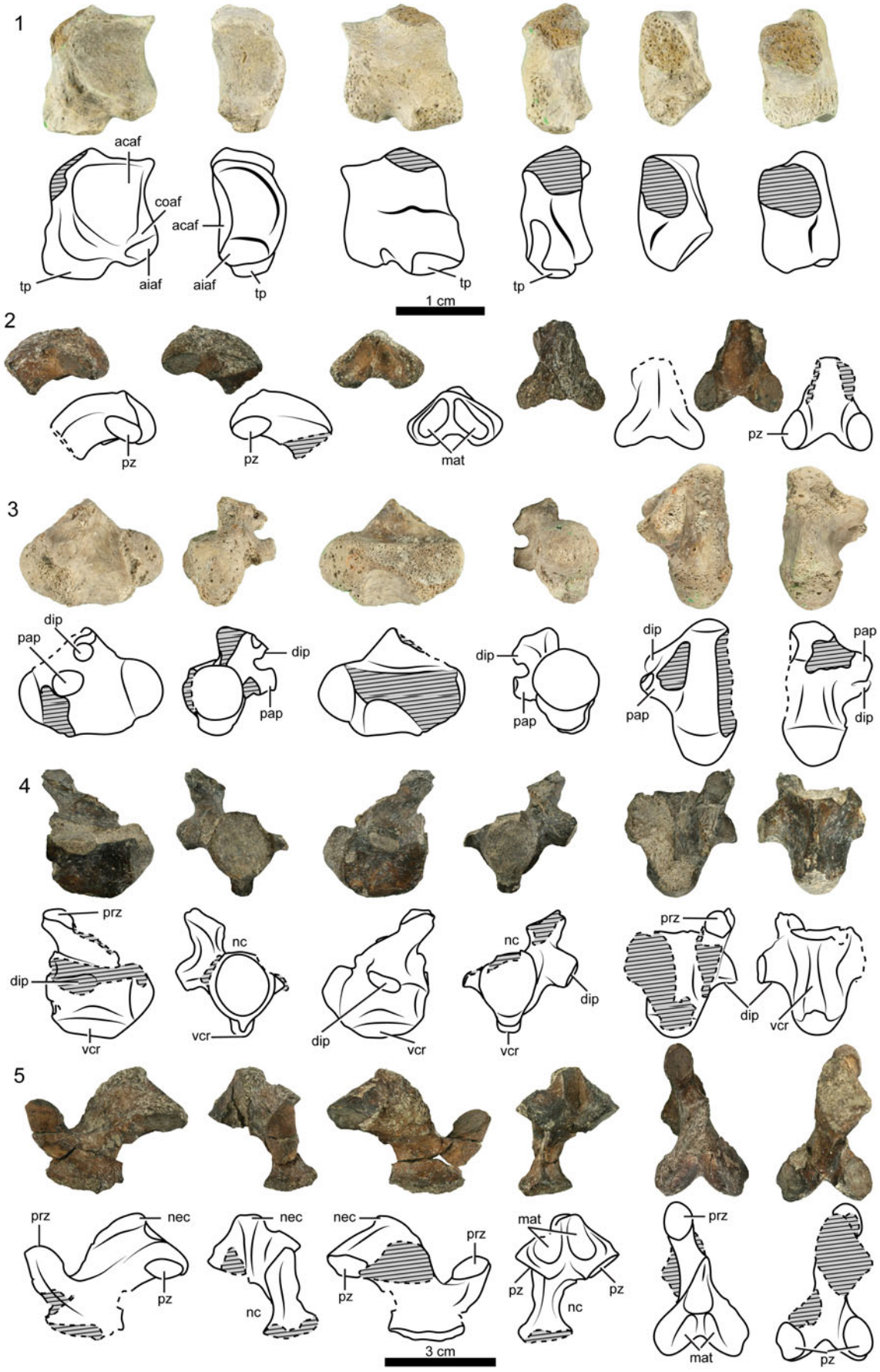


https://doi.org/10.1017/jpa.2019.11 Published online by Cambridge University Press

**Figure 7.** *Peligrochelys walshae* from the Salamanca Formation, Danian, Chubut Province, Argentina. Pictures and drawings of (**1**) the left neural arch of the atlas (MPEF-PV 10832) in medial, anterior, lateral, posterior, dorsal, and ventral views; (**2**) neural arch of cervical vertebra 3 (MPEF-PV 10831) in left lateral, anterior, right lateral, posterior, dorsal, and ventral views; (**3**) cervical vertebra 4 (MPEF-PV 10913) in left lateral, anterior, right lateral, posterior, dorsal, and ventral views; (**4**) cervical vertebra 5 (MPEF-PV 10831) in left lateral, anterior, right lateral, posterior, dorsal, and ventral views; (**5**) neural arch of cervical vertebra 7 (MPEF-PV 10831) in left lateral, anterior, right lateral, posterior, dorsal, and ventral views. Scale bars are 1 cm (**1**) and 3 cm (**2–5**). Black, continuous lines indicate natural borders and sutures. Black, dashed lines indicate broken edges. Diagonal pattern indicates broken bone. Spotted pattern indicates sediment. Abbreviations: acaf, atlas centrum articular facet; aiaf, atlas intercentrum articular facet; coaf, condylus occipitalis articular facet; dip, diapophysis; mat, muscular attachment; nec, neural crest; nc, neural canal; pap, parapophysis; prz, prezygapophysis; pz, postzygapophysis; tp, transverse process; vcr, ventral crest.

*Neural.*—Four neural bones (MPEF-PV 10831–10833) are preserved. Neural MPEF-PV 10831 is a rectangular neural bone (Fig. 6.3). Because it is crossed by an intervertebral sulcus, it likely represents neurals 1, 3, 5 (or 6), or 8. The sulcus has in the midline an anterior inflection. Neural MPEF-PV 10833 is hexagonal (Fig. 6.4). It is wider than long and it has anterior short sides. It has a medial keel and is crossed with a sulcus separating two vertebrals. A medial keel is not recognized in other meiolaniforms where at least some neural bones are preserved (e.g., *Ch. copelloi*, *Pa. gasparinae*, *Otwayemys cunicularius* Gaffney et al., 1998). The sulcus has an anterior flexure in the midline. Neurals MPEF-PV 10832 have the sulcus separating vertebrals, and they have a medial keel. Due to the nature of preservation, the shape of the neurals cannot be assessed.

*Peripherals.*—All the peripherals are divided in the middle by the sulcus between marginals. The anterior half of the peripheral is thicker than the posterior part.

One left (MPEF-PV 10831; Fig. 6.5) and four right (MPEF-PV 10831, 10833, 10923, and 10840) peripherals 1 are preserved. They contact the nuchal medially and peripheral 2 laterally. Other contacts are difficult to determine.

One left peripheral 2 (MPEF-PV 10831) is preserved. The only preserved contact is the medial one with peripheral 1.

Three left (MPEF-PV 10836, 10840, and 10911) and three right (MPEF-PV 10831, 10834, 10911) peripherals 3 are preserved. In peripheral 3, the bridge starts. In medial view, the socket for the reception of the plastron (ventrally) and the rib (dorsally) are seen. The peripheral is crossed by a sulcus separating marginal scales 3 and 4.

A bridge peripheral (MPEF-PV 10904), an anterior right bridge peripheral (MPEF-PV 10904), a right bridge peripheral (MPEF-PV 10836), a left bridge peripheral (MPEF-PV 10906), and two left, last bridge peripherals (MPEF-PV 10831, 10836) are preserved. The bridge peripheral is L-shaped. The sockets for the plastron and ribs are seen in medial view.

There are some peripherals (free peripherals and from the bridge) in specimen MPEF-PV 10832. The peripherals have the sulcus between the marginal, as the typical shape found in other meiolaniforms; they are markedly curved anteriorly.

*Plastron.*—There are several plastral remains preserved in specimens MPEF-PV 10831 and 10832. However their poor preservation does not allow any further description.

*Vertebral column.*—Remains of cervical, thoracic, sacral, and caudal vertebrae are known for *P. walshae*.

*Cervical vertebrae (Fig. 7).*—At least five of the eight cervical vertebrae of the neck in *P. walshae* are preserved (remains of atlas, third, fourth, fifth, and seventh). They were not found in articulation, and some of them belong to more than one specimen (e.g., two remains correspond to cervical vertebra 2, three centra correspond to cervical vertebra 4, two cervical correspond to vertebra 5). A medial keel is not recognized in other meiolaniforms where at least some neural bones are preserved (e.g., *Ch. copelloi*, *Pa. gasparinae*, *O. cunicularius*). Based on the principles of comparative anatomy applied for the cervical vertebrae of *P. walshae*, we suggest that the cervical formula for this species was: ?1? ?2((3((4))5) ?6? ?7? ?8).

The ?left neural arch of the atlas is preserved in specimen MPEF-PV 10832 (Fig. 7.1). In anterior view, the articulation facet with the occipital condyle is seen. Ventrally there is a small facet for the articulation with the intercentrum of the atlas. In medial view, the articulation with the centrum of the atlas is seen. In lateral view, in the posteroventral corner, there is a process interpreted as the transverse process. Unfortunately, the development of the dorsal portion of the neural arch of the atlas cannot be established with certainty because this area is broken in the specimen.

The left half of an opisthocoelous centrum (MPEF-PV 10832) corresponding to cervical vertebra 3 is preserved. Comparisons with *Pa. gasparinae* allow us to suggest this vertebra could correspond to the third cervical vertebrae. The anterior condyle is triangular, while the posterior cotyle is round. The centrum is longer than high and it is compressed ventrally, forming a ventral ridge slightly protruding beyond the centrum. The diapophysis is located in the anterior part of the centrum almost reaching the condyle. The parapophysis is located in the posteroventral part of the centrum.

Much of the posterior part of the neural arch of the cervical vertebra 3 (MPEF-PV 10831) is preserved (Fig. 7.2). The postzygapophysis points ventrolaterally. In posterior view and above the postzygapophysis, there are two concavities separated by a vertical ridge, as in *Pa. gasparinae*. These concavities could be related with the insertion of semispinalis muscled (Shah, 1963).

There are three cervical centra (MPEF-PV 10913, 10914, 10917) recognized as cervical vertebra 4. The centrum is biconvex, longer than high (Fig. 7.3). The anterior condyle is round in outline, while the posterior one is oval, higher than wide. Ventrally, the centrum is constricted, ending in a ridge, and below the posterior condyle it bears a rugose area. This ventral ridge does not protrude ventrally to the centrum. In the anterodorsal part of the centrum reaching the border of the anterior condyle, the parapophysis is preserved. The dia- and parapophyses are located in the anterodorsal part of the centrum. The cervical rib is not preserved.

There are three cervical vertebrae identified as cervical 5 (MPEF-PV 10831, 10913, 10921). Cervical vertebra 5 is

https://doi.org/10.1017/jpa.2019.11 Published online by Cambridge University Press

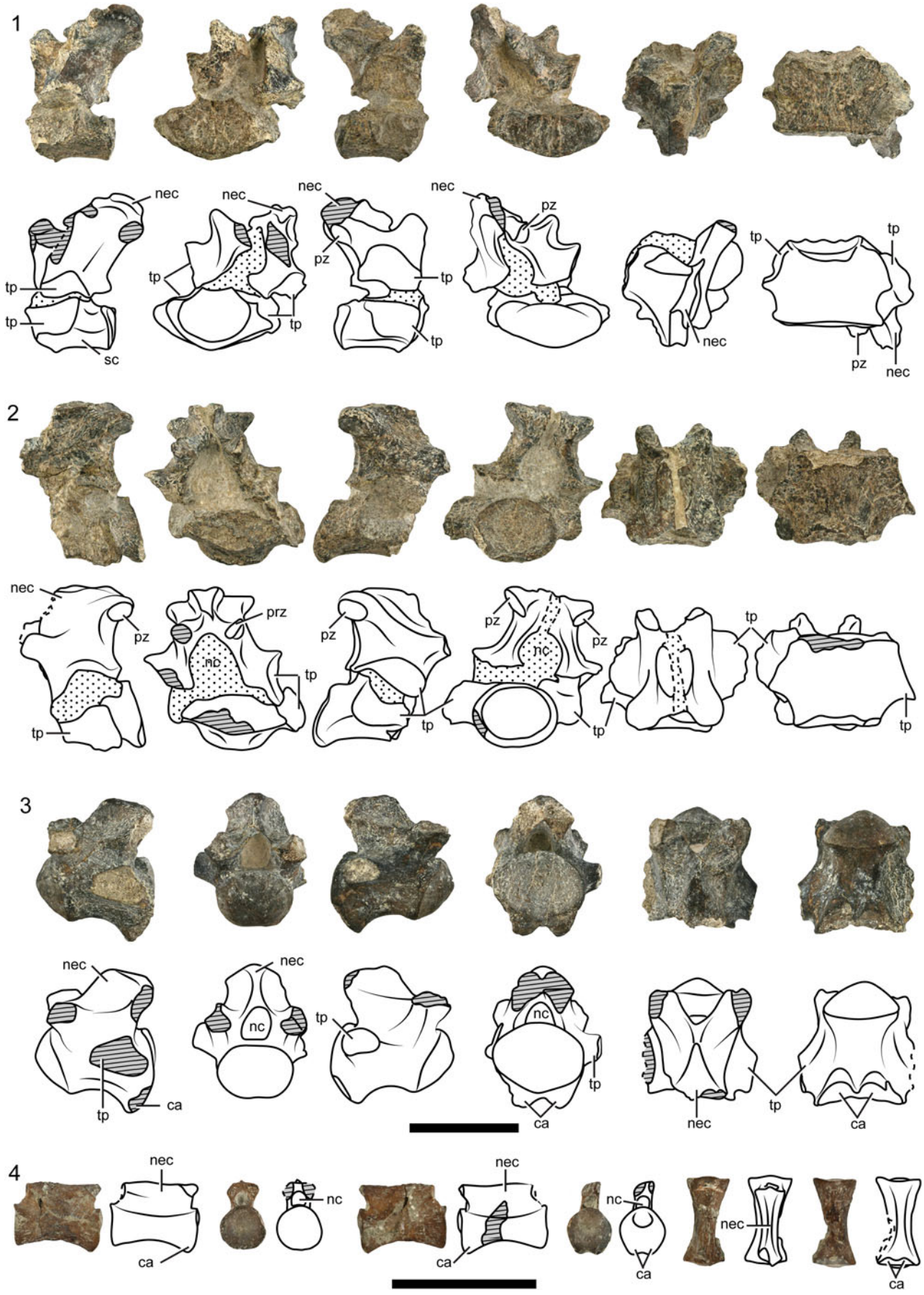


https://doi.org/10.1017/jpa.2019.11 Published online by Cambridge University Press

**Figure 8.** *Peligrochelys walshae* from the Salamanca Formation, Danian, Chubut province, Argentina. Pictures and drawings of (**1**) sacral vertebra 12 (MPEF-PV 10831) in left lateral, anterior, right lateral, posterior, dorsal, and ventral views; (**2**) caudal vertebra 1 (MPEF-PV 10831) in left lateral, anterior, right lateral, posterior, dorsal, and ventral views; (**3**) anterior caudal vertebra (MPEF-PV 10831) in left lateral, anterior, right lateral, posterior, dorsal, and ventral views; (**4**) posterior caudal vertebra in left lateral, anterior, right lateral, posterior, dorsal, and ventral views. Black, dashed lines indicate broken edges. Diagonal pattern indicates broken bone. Spotted pattern indicates sediment. Scale bar represents 3 cm. Abbreviations: ca, chevron articulation; nec, neural crest; nc, neural canal; prz, prezygapophysis; pz, postzygapophysis; sc, sacral centrum; tp, transverse process.

procoelous (Fig. 7.4). Both, the cotyle and condyle are more or less oval in outline, with the cotyle bigger in size. Ventrally, the centrum is constricted, ending in a ridge, which does not protrude ventrally to the centrum. The parapophysis is located in the anteroventral part of the centrum. Contrary to cervical vertebra 4, the parapophysis is not in contact with the border of the cotyle. The left prezygapophysis is small and dorsomedially oriented. The diapophysis is located in the anterodorsal part of the centrum. This diapophysis is broken, but it is dorsoposteriorventroanteriorly oriented.

Most of the neural arch of the cervical vertebra 7 (MPEF-PV 10831) is preserved, only missing the right prezygapophysis (Fig. 7.5). It is a very tall arch. The prezygapophysis is well developed, round, and pointing dorsomedially. The postzygapophysis is also round, pointing ventrolaterally. The neural arch has a blunt neural crest. Between the neural crest and the postzygapophysis in posterior view, there are two elongated concavities separated by a ridge. These concavities could be related with the insertion of longissimus thoracis muscle (Shah, 1963).

A half part of a cervical centrum is recognized in specimen MPEF-PV 10840. It bears a condyle, which is taller than wide. Ventral to the condyle, there is a rugose surface that may have been for muscle attachment. Unfortunately we cannot determine which cervical vertebra it is.

*Thoracic vertebrae.*—A mid-thoracic vertebra is recognized in MPEF-PV 10831. It is a long, slender thoracic vertebra, identified as belonging to the middle part of the column. Only one articular facet is preserved, and it is platycoelous. The body of the vertebra is tall and narrow, and the articular facet is taller than wide.

Comparison with the well-known thoracic vertebral column of *Pa. gasparinae* allowed us to recognize the presence of a thoracic vertebra 9 for *Pe. walshae*. Thoracic vertebra 9 (MPEF-PV 10831) is shorter than the previously described vertebra. Thoracic vertebra 9 is platycoelous and the articular surfaces are wider than high, with the posterior one wider than the anterior one. The anterior two-thirds of the centrum are attached to the thoracic rib (probably the ninth).

*Sacral vertebrae (Fig. 8.1).*—Only sacral vertebra 2 is known for *P. walshae*. They are similar in morphology to *Pa. gasparinae* (Sterli and de la Fuente, 2011b, fig. 9 A–B). The sacral formula suggested for *P. walshae*: ?sa1| |sa2|, where "|" denotes synchondrosis.

Three sacral vertebrae 2 (MPEF-PV 10831, 10834, 10840) are preserved. The centrum of sacral 2 is very flat, being much wider than long (Fig. 8.1). Sacral 2 is slightly concave anteriorly and platycoelous posteriorly (to contact through synchondrosis caudal vertebra 1). The posterior articulating surface is more than two times wider than high. The sacral rib is attached in the anterior two-thirds of the centrum. The neural arch is preserved, although it is displaced from its natural position. It is high with a blunt neural crest towards the posterior part of the arch. Only the right postzygapophysis is preserved, and it is reduced.

Conversely to *Pe. walshae*, sacral vertebrae 1 and 2 in *Naomichelys speciosa* are procoelous, have an hourglass-shaped ventral ridge, and small, blunt dorsal processes (Joyce et al., 2014, fig. 10).

*Caudal vertebrae (Fig. 8.2, 8.3, 8.4).*—Caudal vertebrae are known from several specimens. One specimen (MPEF-PV 10831) preserved 12 caudal vertebrae. The other specimens are represented by six isolated, opisthocoelous caudal vertebrae (MPEF-PV 10835, 10836, 10908, 10909). The description of the caudal vertebrae is based on the most complete specimen and complemented with the other specimens when specified. In MPEF-PV 10831, nine vertebrae are opisthocoelous and two are procoelous; the remaining is only known by a partial neural arch. All the caudal vertebrae bear in their posteroventral rim the double articulation for chevron bones.

There are two caudal vertebra 1 (MPEF-PV 10831, 10835) preserved. The centrum of caudal vertebra 1 is platycoelous anteriorly (to articulate through synchondrosis with sacral vertebra 2) and concave posteriorly (Fig. 8.2). Both articulating surfaces are wider than high. In the anterior two-thirds of the centrum, the rib is located. The neural arch is well preserved, but is displaced from its natural position. It is tall and has a well-developed neural crest with a dorsal and flat surface. Only the left prezygapophysis is preserved. It is small and points dorsomedially. The postzygapophysis is round and points ventrolaterally.

The most anterior vertebrae are opisthocoelous and have well-developed neural arches with certain development of the neural crest (Fig. 8.3). There are many changes that can be observed from anterior to posterior: the general size of the vertebra decreases, the height of the arches decreases relative with the centra, the centra in turns became much longer than high, the transverse processes move posteriorly in the centrum towards the distal part of the tail, the transverse processes also decrease in size until they disappear in the most posterior vertebrae, and the size of the zygapophyses also decreases towards posterior. The procoelous caudal vertebrae are the most posterior ones (Fig. 8.4). Their centra are much longer than high, with a short neural arch, no transverse processes, and the articulation for chevron bones reduced. A biconvex caudal vertebra should have been present to connect the anterior opisthocoelous section of the tail and the posterior procoelous section. In contrast, all *Naomichelys speciosa* caudal centra are amphicoelous (Joyce et al., 2014, fig. 11), as in basal turtles such as *Proganochelys quenstedti* Baur, 1887, *Palaeochersis talampayensis* Rougier,

https://doi.org/10.1017/jpa.2019.11 Published online by Cambridge University Press

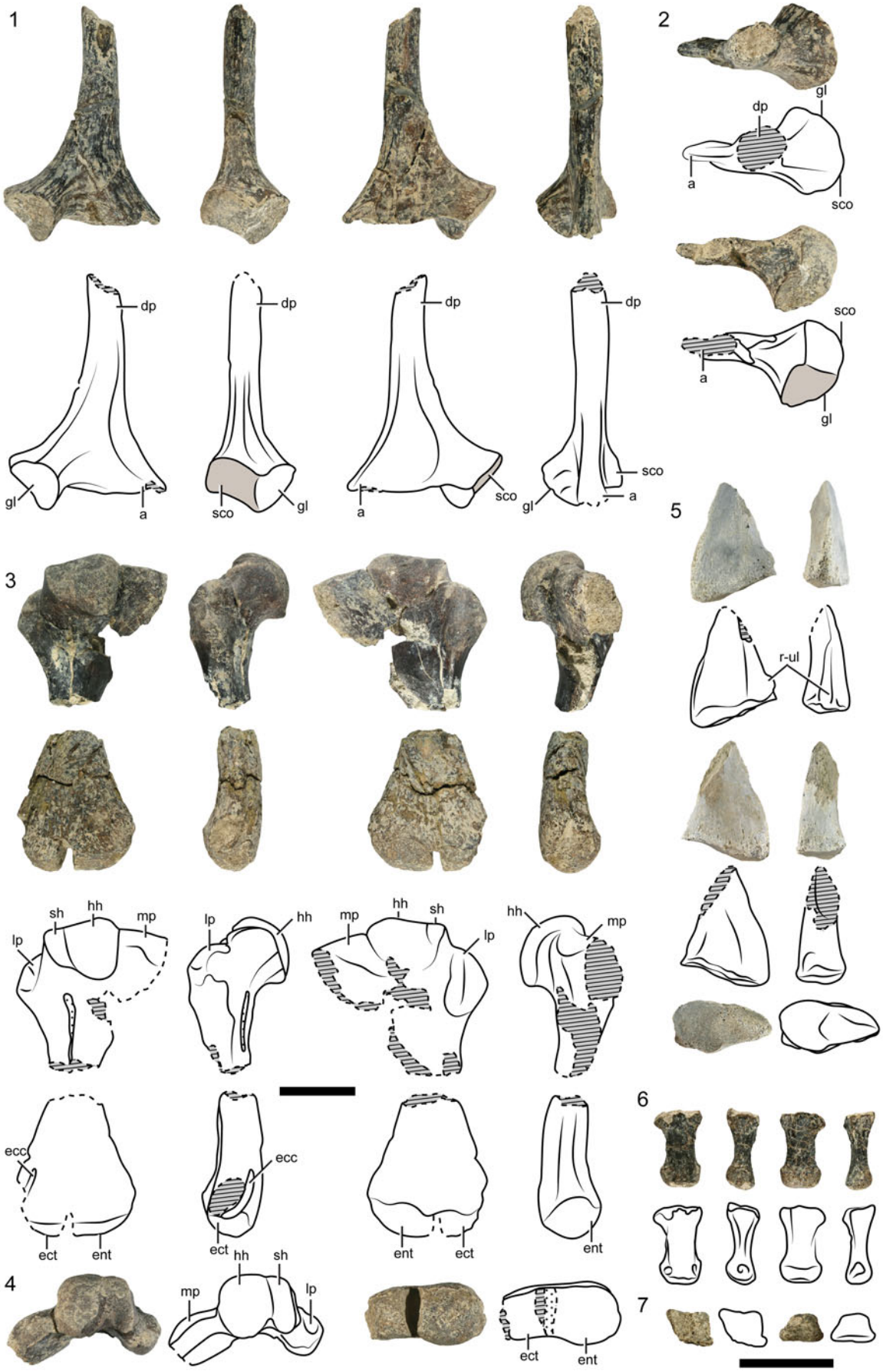


https://doi.org/10.1017/jpa.2019.11 Published online by Cambridge University Press

**Figure 9.** *Peligrochelys walshae* from the Salamanca Formation, Danian, Chubut Province, Argentina. Pictures and drawings of (**1**) right scapula (MPEF-PV 10831) in anterior, lateral, posterior, and medial views; (**2**) right scapula in dorsal and ventral views; (**3**) left humerus (proximal end = MPEF-PV 10915, distal end = MPEF-PV 10831) in dorsal, anterior, ventral, and posterior views; (**4**) left humerus (proximal end = MPEF-PV 10915, distal end = MPEF-PV 10831) in proximal and distal views; (**5**) distal end of left radius (MPEF-PV 10835) in dorsal, lateral, ventral, medial, and distal views; (**6**) metacarpal (MPEF-PV 10831) in dorsal, lateral, ventral, and medial views; (**7**) metacarpal (MPEF-PV 10831) in proximal and distal views. Scale bar represents 3 cm. Black, dashed lines indicate broken edges. Diagonal pattern indicates broken bone. Spotted pattern indicates sediment. Abbreviations: a, acromion; dp, dorsal process of the scapula; ecc, ectepicondylar canal; ect, ectepicondyle; ent, entopicondyle; gl, glenoid; hh, humeral head; lp, lateral process; mp, medial process; r-ul, radio-ulna ligament; sco, suture with coracoid; sh, shoulder.

de la Fuente, and Arcucci, 1995, and *Condorchelys antiqua* Sterli, 2008. The general morphology and the caudal formula of *Pe. walshae* is similar to the caudal formula of *Pa. gasparinae* described by Sterli and de la Fuente (2011b). Conversely, in *Ka. bajazidi*, the caudals are low and wide, the neural spine is a low ridge, and the caudal centra are amphicoelus, except the platycoelous articulation between the first caudal and the last sacral (Gaffney and Meylan, 1992; Pérez-García and Codrea, 2017).

*Pectoral girdle.*—The pectoral girdle in *P. walshae* is triradiate.

*Scapula (Fig. 9.3, 9.4).*—There are two preserved scapulae, one left (MPEF-PV 10831) and one right (MPEF-PV 10834). The dorsal process is long and is round distally. The length of the acromial process cannot be determined. Between the dorsal process and the acromion there is a web of bone, similar to *Mo. efremovi*. The glenoid is rectangular, slightly convex to almost flat, with a medial constriction between the scapula and coracoid. The glenoid neck is present.

*Coracoid.*—Only the proximal end of left coracoid (MPEF-PV 10831) and small portion of a right coracoid (MPEF-PV 10834) are preserved. The coracoid is expanded proximally towards the glenoid. It contacts the scapula and it forms part of the glenoid.

*Forelimb.*—Several remains recognized as part of the forelimb of *P. walshae* are described herein.

*Humerus (Fig. 9.3, 9.4).*—One right (MPEF-PV 10836) and three left (MPEF-PV 10831, 10835, 10915) humeri are preserved. The proximal and distal ends are expanded, the proximal being more expanded than the distal. In the proximal end of the humerus of *P. walshae*, the head, the shoulder, the medial and lateral processes are recognized. The head is well defined and slightly oval. Next to it and towards the lateral side, a well-developed shoulder is present, as seen in *K. bajazidi* and other basal turtles. In general aspects, the medial process is more developed (posteriorly and proximally) than the lateral and more or less continuous with the head. The lateral process, on the contrary, is separated from the head by a notch. In ventral view, the intertubercular fossa is present between the medial and lateral processes. The diaphysis of the humerus is not preserved. The distal end of the humerus bears, in dorsal view, the canal for the foramen ectepicondylar. In the distal end, we can see that the foramen ectepicondylar is enclosed in bone. In ventral view, the distal end of the humerus bears the condyle for the radius (capitellum) anteriorly and the condyle for the ulna (trochlea), posteriorly. The trochlea is bigger than the capitellum in *P. walshae*, contrary to *Pro. quenstedti*. The ectepicondylar canal exits in the ventral view, next to the capitellum.

*Radius.*—The distal end of the left radius is preserved in specimen MPEF-PV 10835 (Fig. 9.5). In the lateral part of the distal end, there is a rugosity for the distal attachment of the radio-ulnar ligament (Gaffney, 1996). The articulation with the carpus is elongated with a pronounced lateroproximal slope.

*Metacarpals (Fig. 9.6, 9.7).*—A left metacarpal III or IV (MPEF-PV 10831) is preserved. It is a robust element, slightly expanded in both ends. The proximal end shows a medioventral process that underlays the previous metacarpal and a laterodorsal process that overlays the next metacarpal.

*Metacarpus/metatarsus.*—A distal portion of a metacarpal/metatarsal (MPEF-PV 10832) is also preserved. The distal end is expanded and it is slightly asymmetrical, suggesting this could belong to the left hand or foot. The articular surface for the phalanx and the concavities for the insertion of tendons are preserved.

*Phalanges.*—There are three preserved phalanges (MPEF-PV 10831, 10832). They are robust elements. Both ends are expanded.

*Ungual.*—Only one ungual phalanx (MPEF-PV 10831) is preserved. It is slightly distorted and the distal end is missing. It is claw-like, triangular in shape, and tall. It is at least two times longer than wide. In one of the sides (the other side is damaged), it has a groove, like in *Mo. efremovi*.

*Hindlimb.*—Several remains recognized as part of the hindlimb of *P. walshae* are described herein.

*Femur.*—Only one right femur (MPEF-PV 10831) is preserved (Fig. 10.1). It is almost complete, only lacking the tip of the distal end. Both ends are expanded and the shaft is round, slender, and slightly curved, as in most turtles. The femur is more than two times longer than wide (measured in the maximum preserved width in the proximal end). The proximal end bears the trochanters and the head. The head is oval and inclined (from posteroproximally to anterodistally). The trochanter major is continuous with the head, while the minor is separated by a notch. Both trochanters are seen in dorsal view. In ventral view, the trochanters border the intertrochanteric fossa. Due to the nature of the specimen, the distal end cannot be described in detail.

*Tibia.*—Only the distal end of the left tibia (MPEF-PV 10831) is preserved (Fig. 10.2). It has medial flat and lateral domed

https://doi.org/10.1017/jpa.2019.11 Published online by Cambridge University Press

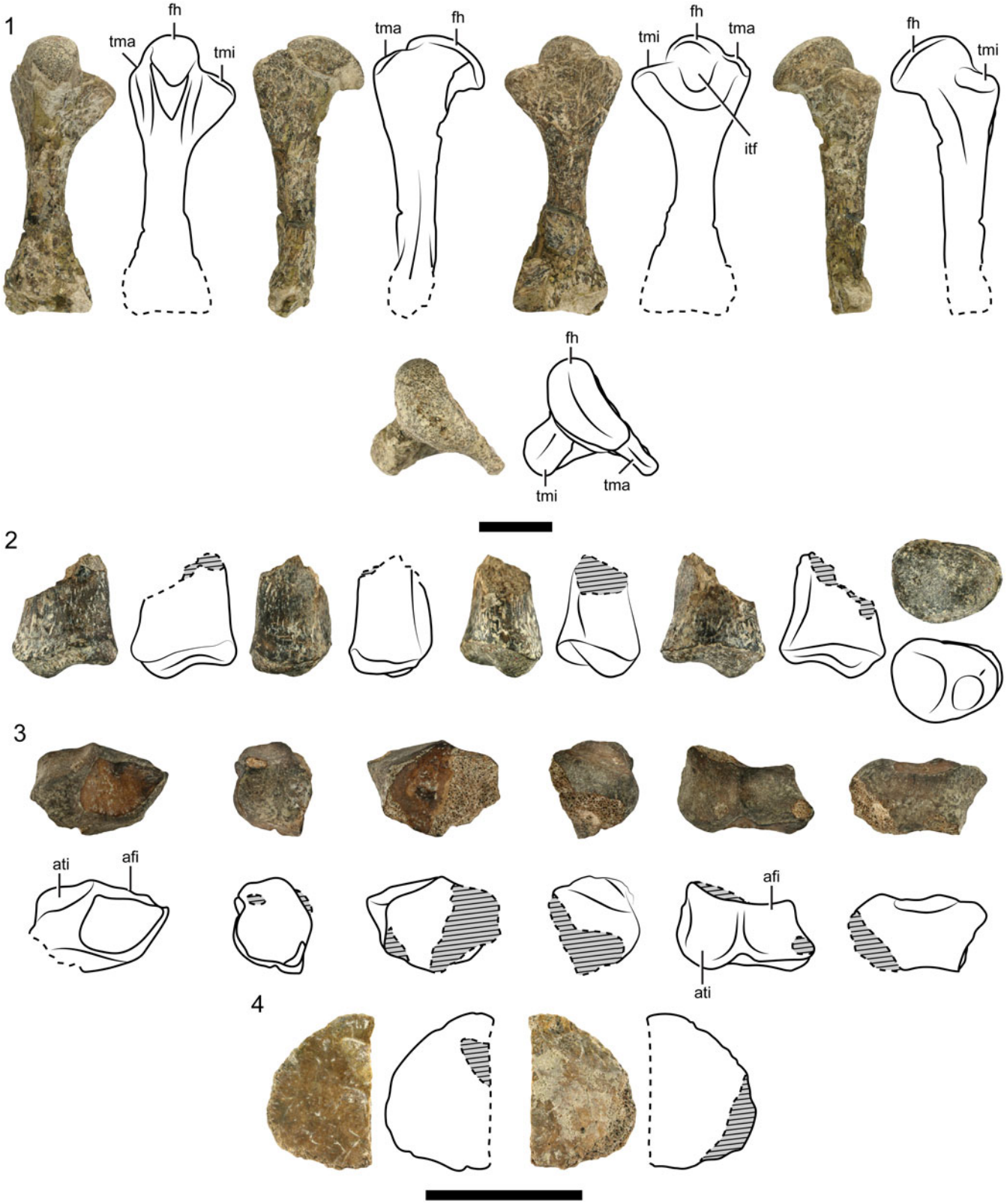


**Figure 10.** *Peligrochelys walshae* from the Salamanca Formation, Danian, Chubut Province, Argentina. Pictures and drawings of (**1**) right femur (MPEF-PV 10831) in dorsal, posterior, ventral, anterior, and proximal views; (**2**) distal end of left tibia (MPEF-PV 10831) in dorsal, medial, lateral, ventral, and distal views; (**3**) left astragalocalcaneum (MPEF-PV 10831) in anterior, lateral, posterior, medial, proximal, and distal views; (**4**) osteoderm (MPEF-PV 10834) in dorsal and visceral views. Black, dashed lines indicate broken edges. Diagonal pattern indicates broken bone. Spotted pattern indicates sediment. Scale bars represent 3 cm (**1**) and (**2–4**). Abbreviations: afi, articulation with fibula; ati, articulation with tibia; fh, femoral head; itf, intertrochanteric fossa; tma, trochanter major; tmi, trochanter minor.

https://doi.org/10.1017/jpa.2019.11 Published online by Cambridge University Press

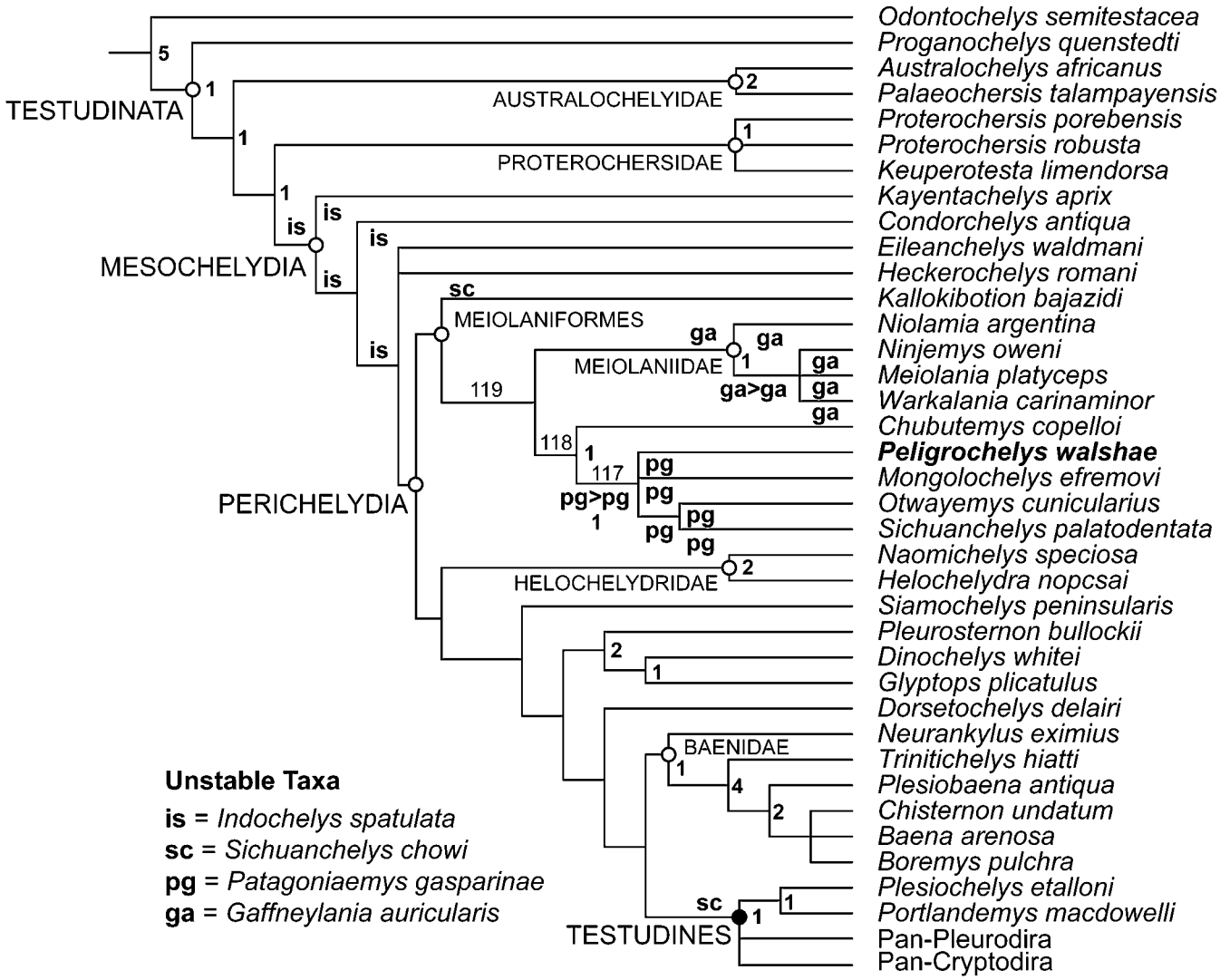


**Figure 11.** Simplified, reduced strict consensus of 10000 most parsimonious trees of 966 steps (CI: 0.327; RI: 0.765); ga, is, pg, and sc indicate the alternate position of the taxa mentioned in the figure; black circle denotes crown-group definition; white circle denotes synapomorphy-based or stem-based group definitions; numbers in bold in the node denote Bremer supports; numbers in regular font denote node number

surfaces for the astragalocalcaneum. The articular surface in distal view is triangular.

*Astragalocalcaneum.*—Only a left astragalocalcaneum (MPEF-PV 10831) is preserved for *P. walshae* (Fig. 10.3). It is almost complete, only missing a portion of the medial part. The astragalus and calcaneum are fused together; no suture between the bones is seen. The astragalocalcaneum is an irregular block-like element. In its proximal surface, the articular surfaces for the tibia (medially) and for the fibula (laterally) are preserved. Both surfaces are separated by a blunt ridge. Distally, the astragalocalcaneum bears the articular surface for the tarsals. In anterior view, this bone has a shallow concavity on the lateral half, while in the medial half, it has a bump.

*Osteoderm.*—A part of an osteoderm is preserved in specimen MPEF-PV 10834 (Fig. 10.4). It is a thin element ornamented with small pits randomly arranged.

## Results of the phylogenetic analyses

The Traditional Search algorithm only hit the minimum length 17 times in 1000 replicates. Consequently, we ran the New Technology Search. With NTS the minimum length was hit 30 times. After a second round of TBR, 10000 trees (tree memory set on 10000 trees) of 966 steps were found (CI: 0.327; RI: 0.765; Supplementary Data 7). A strict consensus of all most parsimonious trees (MPTs) was calculated (see Supplementary Data 8). Because there were some polytomies in the strict consensus tree, the "pruned tree" tool of TNT suggested some wildcard taxa. Because we were more interested in the base of the tree and the tool recognized *Indochelys spatulate* Datta et al., 2000, *Sichuanchelys chowi* Ye and Pi, 1997, *Patagoniaemys gasparinae*, and *Gaffneylania auricularis* Sterli, de la Fuente, and Krause, 2015b among the wildcard taxa, we calculated reduced strict consensus. A simplified, reduced strict consensus tree is shown in Figure 11.

https://doi.org/10.1017/jpa.2019.11 Published online by Cambridge University Press

The general topology of the simplified, reduced strict consensus resembles previously published phylogenies of turtles (e.g., Joyce, 2007; Anquetin, 2010; Sterli et al., in press) with a highly populated stem lineage. However, some differences exist with previously published papers. Focusing on the main topic of this manuscript, we present the results regarding *Peligrochelys walshae* and related taxa. Contrary to recently published papers on general turtle evolution (e.g., Joyce et al., 2016; Pérez-García and Codrea, 2017), we recovered the clade Meiolaniformes as including Meiolaniidae, *Kallokibotion bajazidi*, *Chubutemys copelloi*, *Patagoniaemys gasparinae*, *Peligrochelys walshae*, *Mongolochelys efremovi*, and "*Sichuanchelys*" *palatodentata* Joyce et al., 2016. Because this clade is not recovered in the strict consensus tree (because *Sichuanchelys chowi* jumps between *K. bajazidi* and near the node Testudines, see Fig. 11), there are no synapomorphies common to all trees supporting it. The most basal taxon of this clade is *K. bajazidi*, which is the sister group of a clade (node 119) formed by two monophyletic groups, Meiolaniidae and the remaining meiolaniforms. This arrangement inside Meiolaniformes is different from previous analyses (e.g., Sterli and de la Fuente, 2011b; Sterli et al., 2015a) where non-meiolaniid meiolaniforms were recovered as a paraphyletic group in the stem of Meiolaniidae. Node 119 is supported by three common synapomorphies present in all trees: long posterior entoplastral process [ch. 151 (0)], formed cervical articulation [ch. 195 (1)], and formed caudal articulation [ch. 209 (1)], and 1 synapomorphy present in some trees: small protuberances in the squamosal [(ch. 26 (1)]. The clade Meiolaniidae is supported by seven synapomorphies common to all trees: quadratojugal-squamosal contact below cavum tympani [(ch. 23 (1)], big protuberances in the squamosal developed as big horns [ch. 26(2)], basipterygoid process absent and sutured basicranial articulation [ch. 59 (2)], interpterygoid vacuity reduced to an intrapterygoid slit [ch. 60 (1)], canalis carotici interni posterior to bifurcation in arteria cerebralis and arteria palatina covered ventrally by bone [ch. 97 (1)], arteria palatina entering the skull through the interpterygoid slit [ch 98(0)], and foramen posterius canalis carotici interni formed by pterygoid [ch. 99(1)]. This clade is also supported by seven synapomorphies present in some trees, such as small protuberances in the squamosal [(ch. 25(1)], antrum postoticum absent [ch. 51(0)], Eustachian tube enclosed in bone [ch. 53(1)], large exposure of the supraoccipital in the skull roof [ch. 73(1)], scale F formed by only one scale [ch. 115(1)], tail club present [ch. 208(0)], and tail rings present [ch. 213(1)], and it has a Bremer support of 1.

Clade 118 (Fig. 11) is supported by three synapomorphies common to all trees: cranioquadrate space covered ventrally by pterygoid but pterygoid not covering the prootic [(ch. 48(1)], pterygoid-basioccipital contact absent [ch. 62(0)], and processus pterygoideus externus as in *Proganochelys quenstedti* [ch. 70(0]. It has a Bremer support of 1. In this clade, *Chubutemys copelloi* is the sister taxon of node 117. Node 117 is supported by 1 synapomorphy common to all trees: nuchal emargination including peripheral 1 [(ch. 243(2)], and one synapomorphy present in some trees: paired pits present in the basisphenoid and developing posteriorly reaching the basioccipital [(ch. 84(2)], and it has a Bremer support of 1. A complete list of synapomorphies common to all trees is provided in Supplementary Data 1.

Different positions of *Indochelys spatulata* cause the polytomy in Mesochelydia in node 114 of the strict consensus. Different positions of *Sichuanchelys chowi* cause the big polytomy in node 116, when *S. chowi* is excluded from the strict consensus, this polytomy is resolved and *K. bajazidi* is recovered as the most basal taxon of Meiolaniformes (Fig. 17). It is interesting to note is that *S. chowi* does not jump as a sister taxon of "*S.*" *palatodentata*, for this reason we use "*S.*" *palatodentata* between quotation marks. Different positions of *Patagoniaemys gasparinae* cause the polytomy inside node 117. Also, *Gaffneylania auricularis* was recovered as a wildcard taxon and it is causing the polytomy in Meiolaniidae. Their exclusion from the strict consensus tree (not from the phylogenetic analysis per se) using the command "nelsen//" helps to improve the resolution of the strict consensus tree.

The calibrated topology of the consensus tree (not shown) suggests the presence of several ghost lineages in Meiolaniformes. This is mainly caused by the derived position of some of the oldest members, such as "*S.*" *palatodentata* and *Otwayemys cunicularius*. New data about *Patagoniaemys gasparinae* (under study) and about the fragmentary *O. cunicularius*, and a detailed description of *M. efremovi*, should help to better understand the anatomy and evolution of this clade of turtles.

## Discussion

*Meiolaniformes, a gondwanan or a more distributed clade?*—Meiolaniformes was original defined as "stem-based definition of Meiolaniidae. Meiolaniformes refers to all the taxa more related to *Meiolania platyceps* than to Cryptodira or Pleurodira in the phylogeny shown in Figure 3" (Sterli and de la Fuente, 2013, p. 839). According to that phylogeny, this definition contained the following taxa "the clade Meiolaniidae (which includes *Niolamia argentina* Ameghino, 1899, *Ninjemys oweni* (Woodward, 1888), *Warkalania carinaminor* Gaffney, Archer & White, 1992 and *Meiolania platyceps*) and their stem taxa *Chubutemys copelloi*, *Otwayemys cunicularius*, *Patagoniaemys gasparinae*, *Mongolochelys efremovi*, *Kallokibotion bajazidi* and *Peligrochelys walshae*" (Sterli and de la Fuente, 2013, p. 839). The clade Meiolaniformes in this context, although mainly grouping Gondwanan forms, also contained two Laurasian species (*M. efremovi* and *K. bajazidi*). Posterior phylogenetic analyses performed by Sterli and de la Fuente (e.g., Sterli et al., 2015a; Sterli and de la Fuente, in press) also showed Meiolaniformes containing Gondwanan and Laurasian representatives.

Recently, new phylogenetic hypotheses (Joyce et al., 2016; Pérez-García and Codrea, 2017) have challenged the composition of Meiolaniformes as originally defined, and obtained *M. efremovi* and *K. bajazidi*, as well as the recently described species "*S.*" *palatodentata*, outside Meiolaniformes and in more derived positions in the turtle tree. These new hypotheses have some paleobiogeographic implications. In this case, Meiolaniformes only contains Gondwanan representatives. Although this later hypothesis could imply less "ad hoc" paleobiogeographical events, it shows a long ghost lineage (ca. 85 My) between the Oxfordian "*S.*" *palatodentata* and the Maastrichtian *M. efremovi*.

The results of the phylogenetic analysis presented here suggest that Meiolaniformes also includes Laurasian taxa, as was

https://doi.org/10.1017/jpa.2019.11 Published online by Cambridge University Press

originally suggested. To further explore the alternate hypotheses about this clade, we performed a Templeton test. The results of this test are discussed below.

*Exploring alternate positions of* "Sichuanchelys" palatodentata, Mongolochelys efremovi, *and* Kallokibotion bajazidi.—A recent phylogenetic analysis suggested that *Sichuanchelys chowi*, "*S*." *palatodentata*, and *Mongolochelys efremovi* form a clade (Sichuanchelyidae) outside Meiolaniformes and located in a more derived position (Joyce et al., 2016). Furthermore, a more derived position outside Meiolaniformes was also recently suggested for *Kallokibotion bajazidi* (Joyce et al., 2016; Pérez-García and Codrea, 2017). In our analysis, we included the new anatomical information available for *K. bajazidi*, thanks to the work of Pérez-García and Codrea (2017), and we modified several characters accordingly (Supplementary Data 1). We also incorporated "*S*." *palatodentata* into the analysis and all characters we considered appropriate to explore the phylogenetic relationships of all these basal turtles (see Supplementary Data 1 for all the aspects concerning the building of the matrix). Because our analysis recovered these three taxa within Meiolaniformes, we utilized a Templeton test to test whether alternative placements are statistically significant.

The constrained analysis (considering "*S*." *palatodentata*, *M. efremovi*, and *K. bajazidi* outside Meiolaniformes, as in Joyce et al., 2016 and Pérez-García and Codrea, 2017) resulted in 10000 trees (maximum tree memory) of 976 steps, 10 steps longer than the most parsimonious trees (Supplementary Data 9). Under parsimony, there is no doubt that the unconstrained analysis is the chosen one because it is shorter than the constrained analysis. However, to test whether the topological differences between unconstrained and constrained analyses are statistically significantly different, we ran a Templeton test using one of the most parsimonious trees and one of the suboptimal, constrained trees randomly selected (Supplementary Data 10). The result of this test (Supplementary Data 11) suggests that both hypotheses are statistically not significantly different from each other and that the present data set could support both alternate hypotheses. Both constrained and unconstrained randomly selected trees differ in the optimization of 31 characters, 19 (18 with one step and one with two steps) perform better in the unconstrained tree, and 11 perform better in the constrained tree. Although both trees differ in the optimization of 31 characters, the differences are not statistically significantly different following the Templeton Test (sum of negative ranks 170.5, critical value = 163 for the 5% confidence interval; Supplementary Data 11). Note, however, that the sum of the negative ranks is quite close to the critical value—if the constrained tree were just two more steps longer (for the same set of 31 characters), the difference between the two trees would be significant at the 5% level.

As is obvious from the latest phylogenetic analyses, we are still far away from a stable, consensus phylogeny for this part of the turtle tree (around Perichelydia clade). This is mainly due to the fact that there are still some taxa that need a more detailed description (e.g., *M. efremovi*), taxa with new information, but not yet described in detail (e.g., *Pa. gasparinae*), or taxa with limited, available information (e.g., *S. chowi*). Hopefully, new information about those taxa will help to stabilize the phylogeny near clade Perichelydia.

*The survivorship of Meiolaniformes to the K-Pg extinction and the importance of* P. walshae *in this context.*—In this section, we highlight the importance of the finding of *P. walshae* regarding the fossil record of Meiolaniformes and their evolution. First, up to now, *P. walshae* is the most abundant meiolaniform in the fossil record, with almost 30 occurrences in Punta Peligro area (Chubut, Argentina). This is a result of systematic field work performed in the area mainly during 2013 and 2014. Second, the lineage leading to *Peligrochelys walshae* is the only meiolaniform non-meiolaniid lineage that survived the K-Pg mass extinction. According to the phylogeny presented here, the other lineage that survived the K-Pg boundary is the lineage leading to Meiolaniidae, however anatomical and phylogenetic studies of poorly known or studied meiolaniform taxa (e.g., *Pa. gasparinae*, *O. cunicularius*, *M. efremovi*) could change this scenario. A recently published paper about the diversity of South American turtles (Vlachos et al., 2018) suggested, contrary to the observations for North American turtles (e.g., Holroyd and Hutchison, 2002; Hutchison and Holroyd, 2003; Lyson et al., 2011; Holroyd et al., 2014), that turtles in South America were seriously affected by the K-Pg mass extinction and that they continued suffering until mid-late Eocene. Meiolaniformes, in particular, suffered some extinction events in the Aptian, K-Pg boundary, and Paleocene in South America (Vlachos et al., 2018); however, they managed to survive the K-Pg mass extinction and their derived clade, the Meiolaniidae, survived until the Holocene in Australasia (Gaffney et al., 1984). Because *P. walshae* was found in sediments of Danian age, Punta Peligro represents an important area to explore the aftermath of the K-Pg extinction on turtles. From the same area, at least three species of chelid turtles are known: *Yaminuechelys maior* (Staesche, 1929), *Salamanchelys palaeocenica* Bona, 2006, and cf. *Hydromedusa* sp. (Bona and de la Fuente, 2005; Bona, 2006; Maniel and de la Fuente, 2016), making Punta Peligro area a highly diverse spot for turtle fauna after this extinction event. Systematic and interdisciplinary field work in the area will bring valuable information about not only the turtle fauna, but also the accompanying fauna (e.g., mammals, crocodiles), and the environment in which they were living. This information will help to better understand the outcome of the K-Pg mass extinction in a holistic approach.

## Conclusions

The new specimens of *P. walshae* from the Danian of Punta Peligro (Chubut, Argentina) bring valuable information about the only known meiolaniform non-meiolaniid from the Cenozoic lineage that survived the K-Pg mass extinction. Previously, *P. walshae* was only known from cranial remains. In this contribution we present new information about cranial and postcranial remains for this species. The bones of the skull and lower jaw of *P. walshae* were 3D scanned and a 3D reconstruction of them is presented for the first time. This 3D reconstruction helps to understand the cranial anatomy of this species and allows seeing the bones in different angles. Considering all the available anatomical information for *P. walshae*, we emended the diagnosis of the species. Furthermore, we tested its phylogenetic position among turtles and we confirm its

https://doi.org/10.1017/jpa.2019.11 Published online by Cambridge University Press

relationships with the clade Meiolaniformes. Our updated phylogeny confirms that Meiolaniformes contains both Gondwanan and Laurasian taxa, a point of debate in recent literature. Compared to our preferred, and most parsimonious, phylogeny, a tree with Meiolaniformes of purely Gondwanan composition would be, at least, 10 steps longer. However, this suboptimal solution (under parsimony) is not significantly different from a statistical point of view. Further information about the anatomy of the members of Meiolaniformes and taxa at the base of Perichelydia would probably help to stabilize turtle phylogeny in this part of the tree.

## Acknowledgments

We thank the Willatowski brothers for their hospitality and help while doing field-work in the area and the people involved in 2013 and 2014 field seasons: F. Barrios, W. Clyde, M. Iberlucea, M. Krause, I. Maniel, L. Nicoli, C. Oriozabala, and P. Puerta. We are also grateful to L. Reiner (MPEF) for preparing the specimens and L. Mollo and J. García Díaz for 3D scanning the specimens and making the 3D reconstruction of the skull and lower jaw. We also thank E. Ruigómez who provided access to the specimens housed at MPEF. The Secretaría de Cultura de Chubut gave permission to work in the area. The revisions of W.G. Joyce and A. Pérez-García highly improved the quality of this paper, as well as the editorial work of H.-D. Sues. This work has been partially financed by PICTs 2012–0227 (JS) and 2013–0095 (MdlF), and PIP-CONICET 00795 (MdlF).

## Accessibility of supplemental data

Data available from the Dryad Digital Repository: https://doi.org/10.5061/dryad.b8g83bc

*Supplementary Data 1*. List of specimens used in this work; list of 3D scanned specimens; construction of the phylogenetic matrix; list of synapomorphies common to all most parsimonious trees.

*Supplementary Data 2*. 3D reconstruction of *Peligrochelys walshae* skull.

*Supplementary Data 3*. Morphological matrix in nexus format.

*Supplementary Data 4*. Morphological matrix in tnt format.

*Supplementary Data 5*. Constraints used in the constrained analysis based on Joyce et al. (2016) and Pérez-García and Codrea (2017).

*Supplementary Data 6*. Script of Templeton test.

*Supplementary Data 7*. Most parsimonious trees in ctf format (for TNT).

*Supplementary Data 8*. Strict consensus tree of 10.000 most parsimonious trees of 966 steps found in the unconstrained analysis.

*Supplementary Data 9*. Most parsimonious trees in ctf format (for TNT) of the constrained analysis.

*Supplementary Data 10*. One most parsimonious tree selected at random and one constrained tree selected at random in ctf (for TNT) used to run the Templeton test.

*Supplementary Data 11*. Result of the Templeton test.

## References

Ameghino, F., 1899, Sinopsis geológica paleontológica. Suplemento (adiciones y correcciones): La Plata, Censo Nacional, 13 p.

Anquetin, J., 2010, The anatomy of the basal turtle *Eileanchelys waldmani* from the Middle Jurassic of the Isle of Skye, Scotland: Earth and Environmental Science Transactions of the Royal Society of Edinburgh, v. 101, p. 67–96.

Anquetin, J., Tong, H., and Claude, J., 2017, A Jurassic stem pleurodire sheds light on the functional origin of neck retraction in turtles: Scientific Reports, v. 7, / e 42376.

Baur, G., 1887, Ueber den Ursprung der Extremitäten der Ichthyopterygia: Bericht des Oberrheinischen Geologischen Vereins, v. 20, p. 17–20.

Bona, P., 2006, Paleocene (Danian) chelid turtles from Patagonia, Argentina: taxonomic and biogeographic implications: Neues Jahrbuch für Geologie und Paläontologie—Abhandlungen, v. 241, p. 303–323.

Bona, P., and de la Fuente, M.S., 2005, Phylogenetic and paleobiogeographic implications of *Yaminuechelys maior* (Staesche, 1929) new comb., a large long-necked chelid turtle from the early Paleocene of Patagonia, Argentina: Journal of Vertebrate Paleontology, v. 25, p. 569–582.

Carballido, J.L., Rauhut, O.W., Pol, D., and Salgado, L., 2011, Osteology and phylogenetic relationships of *Tehuelchesaurus benitezii* (Dinosauria, Sauropoda) from the Upper Jurassic of Patagonia: Zoological Journal of the Linnean Society, v.163, p. 605–662.

Clyde, W.C., Wilf, P., Iglesias, A., Slingerland, R.L., Barnum, T., Bijl, P.K., Bralower, T.J., Brinkhuis, H., Comer, E.E., Huber, B.T., and Ibañez-Mejia, M., 2014, New age constraints for the Salamanca Formation and lower Río Chico Group in the western San Jorge Basin, Patagonia, Argentina: implications for Cretaceous-Paleogene extinction recovery and land mammal age correlations: Geological Society of America Bulletin, v. 126, p. 289–306.

Danilov, I., Syromyatnikova, E., and Sukhanov, V., 2017, Testudinata, *in* Lapatin, A.V., and Zeklenkov, N.V., eds., Fossil Vertebrates of Russia and Adjacent Countries. Fossil Reptiles and Birds. Part 4: Moscow, Russian Academy of Sciences, Borissiak Paleontological Institute Moscow, p. 27–395. [in Russian]

Datta, P.M., Manna, P., Ghosh, S.C., and Das, D.P., 2000, The first Jurassic turtle from India: Palaeontology, v. 43, p. 99–109.

Evers, S.W., and Benson, R.B.J., 2019, A new phylogenetic hypothesis of turtles with implications for the timing and number of evolutionary transitions to marine lifestyles in the group: Palaeontology, v. 62, p. 93–134.

Gaffney, E.S., 1979, Comparative cranial morphology of recent and fossil turtles: Bulletin of the American Museum of Natural History, v. 164, p. 67–376.

Gaffney, E.S., 1983, The cranial morphology of the extinct horned turtle, *Meiolania platyceps*, from the Pleistocene of Lord Howe Island, Australia: Bulletin of the American Museum of Natural History, v. 175, p. 361–480.

Gaffney, E.S., 1985, The cervical and caudal vertebrae of the cryptodiran turtle, *Meiolania platyceps*, from the Pleistocene of Lord Howe Island, Australia: American Museum Novitates, v. 2805, p. 1–29.

Gaffney, E.S., 1996, The postcranial morphology of *Meiolania platyceps* and a review of the Meiolaniidae: Bulletin of the American Museum of Natural History, v. 229, p. 1–166.

Gaffney, E.S., and Meylan, P., 1992, The Transylvanian turtle, *Kallokibotion*, a primitive cryptodire of Cretaceous age: American Museum Novitates, v. 3040, p. 1–37.

Gaffney, E.S., Balouet, J.C., and Broin, F.D., 1984, New occurrences of extinct meiolaniid turtles in New Caledonia: American Museum Novitates, v. 2800, p. 1–6.

Gaffney, E.S., Archer, M., and White, A., 1992, *Warkalania*, a new meiolaniid turtle from the Tertiary Riversleigh deposit of Queensland, Australia: The Beagle, Records of the Northern Territory Museum of Arts and Sciences, v. 9, p. 35–48.

Gaffney, E.S., Kool, L., Brinkman, D.B., Rich, T.H., and Rich, P.V., 1998, *Otwayemys*, a new cryptodiran turtle from the early Cretaceous of Australia: American Museum Novitates, v. 3233, p. 1–28.

Gaffney, E.S., Rich, T.H., Vickers-Rich, P., Constantine, A, Vacca, R., and Kool, L., 2007, *Chubutemys*, a new eucryptodiran turtle from the Early Cretaceous of Argentina, and the Relationships of the Meiolaniidae: American Museum Novitates, v. 3599, p. 1–35.

Goloboff, P., Farris, J.S., and Nixon, K.C., 2003, TNT: Tree Analysis Using New Technology, version 1.1 (Willy Hennig Society Edition). Program and documentation, available at http://www.zmuc.dk/public/phylogeny/tnt.

Goloboff, P., Farris, J.S., and Nixon, K.C., 2008, TNT, a free program for phylogenetic analysis: Cladistics, v. 24, p. 774–786.

Hay, O.P., 1908, The fossil Turtles of North America: Carnegie Institution of Washington, Publication 75, 568 p.

Holroyd, P.A., and Hutchison, J.H., 2002, Patterns of geographic variation in latest Cretaceous vertebrates: evidence from the turtle component, *in* Hartman, J.H., Johnson, K.R., and Nichols, D.J., eds., The Hell Creek

https://doi.org/10.1017/jpa.2019.11 Published online by Cambridge University Press

Formation and Cretaceous-Tertiary Boundary in the Northern Great Plains: An Integrated Continental Record of the End of the Cretaceous: Geological Society of America Special Paper 361, p. 177–190.

Holroyd, P.A., Wilson, G.P. and Hutchison, J.H., 2014, Temporal changes within the latest Cretaceous and early Paleogene turtle faunas of northeastern Montana, *in* Wilson, G.P., Clemens, W.A., Horner, J.R., and Hartman, J.H., eds., Through the End of the Cretaceous in the Type Locality of the Hell Creek Formation in Montana and Adjacent Areas: Geological Society of America Special Paper 503, p. 299–312.

Hutchison, J.H., and Holroyd, P.A., 2003, Late Cretaceous and early Paleocene turtles of the Denver Basin, Colorado: Rocky Mountain Geology, v. 38, p.121–142.

Joyce, W.G., 2007, Phylogenetic relationships of Mesozoic turtles: Bulletin of the Peabody Museum of Natural History, v. 48, p. 3–102.

Joyce, W.G., 2017, A Review of the Fossil Record of Basal Mesozoic Turtles: Bulletin of the Peabody Museum of Natural History, v. 58, p. 65–113.

Joyce, W.G., Parham, J.F., and Gauthier, J.A., 2004, Developing a protocol for the conversion of rank-based taxon names to phylogenetically defined clade names, as exemplified by turtles: Journal of Paleontology, v. 78, p. 989–1013.

Joyce, W.G., Sterli, J. and Chapman, S., 2014, The skeletal morphology of the solemydid turtle *Naomichelys speciose* from the Early Cretaceous of Texas: Journal of Paleontology, v. 88, p. 1257–1287.

Joyce, W.G., Rabi, M., Clark, J.M., and Xu, X., 2016, A toothed turtle from the Late Jurassic of China and the global biogeographic history of turtles: BMC Evolutionary Biology, v. 16, p. 1–29. doi: 10.1186/s12862-016-0762-5

Khosatzky, L.I., 1997, Big turtle from the Late Cretaceous of Mongolia: Russian Journal of Herpetology, v. 4, p. 148–154.

Klein, I.T., 1760, Klassification und kurze Geschichte der Vierfüßigen Thiere (translation by F.D. Behn): Lübeck, Jonas Schmidt, 381 p.

Lesta, P. J., and Ferello, R., 1972, Región extrandina de Chubut y norte de Santa Cruz, *in* Leanza, A., ed., Geología Regional Argentina: Córdoba, Academia Nacional de Ciencias de Córdoba, p. 601–654.

Lyson, T.R., Joyce, W.G., Knauss, G.E., and Pearson, D.A., 2011, *Boremys* (Testudines, Baenidae) from the latest Cretaceous and early Paleocene of North Dakota: an 11-million-year range extension and an additional K/T survivor. Journal of Vertebrate Paleontology, v. 31, p. 729–737.

Maddison, W. P., and Maddison, D.R., 2018, Mesquite: a modular system for evolutionary analysis: Version 3.40 http://mesquiteproject.org

Maniel, I.J., and de la Fuente, M.S., 2016, A review of the fossil record of turtles of the clade Pan-Chelidae: Bulletin of the Peabody Museum of Natural History, v. 57, p. 191–227.

Mannion, P.D., Upchurch, P., Barnes, R.N., and Mateus, O., 2013, Osteology of the Late Jurassic Portuguese sauropod dinosaur *Lusotitan atalaiensis* (Macronaria) and the evolutionary history of basal titanosauriforms: Zoological Journal of the Linnean Society, v. 168, p. 98–206.

Nopcsa, F., 1923, On the geological importance of the primitive reptilian fauna of the uppermost Cretaceous of Hungary; with a description of a new tortoise (*Kallokibotion*): Quarterly Journal of the Geological Society, v. 79, p. 100–116.

Owen, R., 1886, Description of some fossil remains of two species of a megalanian genus (*Meiolania*) from "Lord Howe's Island": Philosophical Transactions of the Royal Society, London, v. B179, p. 181–191.

Pérez-García, A., and Codrea, V., 2017, New insights on the anatomy and systematics of *Kallokibotion* Nopcsa, 1923, the enigmatic uppermost Cretaceous basal turtle (stem Testudines) from Transylvania: Zoological Journal of the Linnean Society, v. 182, p. 419–443.

Rougier, G.W., de la Fuente, M.S., and Arcucci, A.B., 1995, Late Triassic turtles from South America: Science, v. 268, p. 855–858.

Shah, R.V., 1963, The neck musculature of a cryptodire (*Deirochelys*) and a pleurodire (*Chelodina*) compared: Bulletin of the Museum of Comparative Zoology, v. 129, p. 343–368.

Staesche, K., 1929, Schildkrötenreste aus der oberen Kreide Patagoniens: Palaeontographica, v. 72, p. 103–112.

Sterli, J., 2008, A new, nearly complete stem turtle from the Jurassic of South America with implications for turtle evolution: Biology Letters, v. 4, p. 286–289.

Sterli, J., 2015, A review of the fossil record of Gondwanan turtles of the clade Meiolaniformes: Bulletin of the Peabody Museum of Natural History, v. 56, p. 21–45.

Sterli, J., and de la Fuente, M.S., 2011a, Re-description and evolutionary remarks on the Patagonian horned turtle *Niolamia argentina* Ameghino, 1899 (Testudinata; Meiolaniidae): Journal of Vertebrate Paleontology, v. 31, p. 1210–1229.

Sterli, J., and de la Fuente, M.S., 2011b, A new turtle from the La Colonia Formation (Campanian–Maastrichtian), Patagonia, Argentina with remarks on the evolution of the vertebral column in turtles: Palaeontology, v. 54, p. 63–78.

Sterli, J., and de la Fuente, M.S., 2013, New evidence from the Palaeocene of Patagonia (Argentina) on the evolution and palaeo-biogeography of Meiolaniformes (Testudinata, new taxon name): Journal of Systematic Palaeontology, v. 11, p. 835–852.

Sterli, J., de la Fuente, M.S., and Umazano, A.M., 2015a, New remains and new insights on the Gondwanan meiolaniform turtle *Chubutemys copelloi* from the Lower Cretaceous of Patagonia, Argentina: Gondwana Research, v. 27, p., 978–994.

Sterli, J., de la Fuente, M.S., and Krause, J.M., 2015b, A new turtle from the Palaeogene of Patagonia (Argentina) sheds new light on the diversity and evolution of the bizarre clade of horned turtles (Meiolaniidae, Testudinata): Zoological Journal of the Linnean Society, v. 174, p. 519–548.

Sterli, J., de la Fuente, M. S., and Rougier, G.W., in press, New remains of *Condorchelys antiqua* (Testudinata) from the early-middle Jurassic of Patagonia: anatomy, phylogeny, and paedomorphosis in the early evolution of turtles: Journal of Vertebrate Paleontology, doi 10.1080/02724634.2018.1480112.

Sukhanov, V.B., 2000, Mesozoic turtles of Middle and Central Asia, *in* Benton, M.J., Shishkin, M.A., Unwin, D.M., and Kurochkin, E.N., eds., The Age of Dinosaurs in Russia and Mongolia: Cambridge, Cambridge University Press, p. 309–367.

Sullivan, P.M., and Joyce, W.G., 2017. The shell and pelvic anatomy of the Late Jurassic turtle *Platychelys oberndorferi* based on material from Solothurn, Switzerland: Swiss Journal of Palaeontology, v. 136, p. 323–343.

Suzuki, S., and Chinzorig, Ts., 2010, A catalog of *Mongolochelys* collected by the HMNS-MPC Joint Paleontological Expedition: Hayashibara Museum Natural Sciences Research Bulletin, v. 3, p. 119–131.

Templeton, A.R., 1983, Phylogenetic inference from restriction endonuclease cleavage site maps with particular reference to the evolution of humans and the apes: Evolution, v. 37, p. 221–244.

Vlachos, E., Randolfe, E., Sterli, J., Leardi, J.M., 2018, Changes in the diversity of turtles (Testudinata) in South America from the Late Triassic to the present: Ameghiniana, v. 55, p. 619–643.

Wagner, A., 1853, Beschreibung einer fossilen Schildkröten undetlicher anderer Reptilien-Überreste aus den lithographischen Schiefern und dem grünen Sandsteine von Kehlheim: Abhandlungen der bayerischen Akademie der Wissenschaften, mathematisch-physikalische Klasse, v. 7, p. 241–264.

Wilson, J., 2002, Sauropod dinosaur phylogeny: critique and cladistic analysis: Zoological Journal of the Linnean Society, v 136, p. 215–275.

Woodward, A.S., 1888, Note on the extinct reptilian genera *Megalania*, Owen and *Meiolania*, Owen: Annals and Magazine of Natural History, v. 6, p. 85–89.

Ye, Y., and Pi, X., 1997, A new genus of Chengyuchelyidae from Dashanpu, Zigong, Sichuan: Vertebrata PalAsiatica, v. 35, p. 182–188. [in Chinese]

Accepted: 3 February 2019